The methyl phosphate capping enzyme Bin3 is a stable component of the fission yeast telomerase holoenzyme

Jennifer Porat[1], Moaine El Baidouri[2,3], Jorg Grigull[4], Jean-Marc Deragon[2,3,5], & Mark A. Bayfield[1*]

1. Department of Biology, York University, Toronto, Canada

2. LGDP-UMR5096, Université de Perpignan Via Domitia, Perpignan, France

3. CNRS LGDP-UMR5096, Perpignan, France

4. Department of Mathematics and Statistics, York University, Toronto, Canada

5. Institut Universitaire de France, Paris, France

*Correspondence: bayfield@yorku.ca (M.A.B.)

Abstract:

The telomerase holoenzyme is critical for maintaining eukaryotic genome integrity. In addition to a reverse transcriptase and an RNA template, telomerase contains additional proteins that protect the telomerase RNA and promote holoenzyme assembly. Here we report that the methyl phosphate capping enzyme (MePCE) Bin3 is a stable component of the *S. pombe* telomerase holoenzyme. Bin3 associates with the telomerase and the U6 snRNA through an interaction with the recently described LARP7 family member Pof8, and we demonstrate that these two factors are evolutionarily linked in fungi. Our data suggest that the association of Bin3 with telomerase is independent of its methyltransferase activity, but rather that Bin3 negatively regulates TER1 levels and telomere length. Taken together, this work yields new

24 insight into the composition, assembly, and regulation of the telomerase holoenzyme in fission
25 yeast as well as the breadth of its evolutionary conservation.
26
27 **Introduction:**
28 To ensure complete DNA replication, the termini of eukaryotic chromosomes contain tandem
29 repeats, or telomeres, that can be continually extended as the ends of linear chromosomes are
30 lost through DNA replication. Telomeres serve as protection from DNA degradation, end-to-end
31 fusions, chromosomal rearrangements, and chromosome loss [1,2]. With very few exceptions,
32 eukaryotes extend telomeric DNA sequences through the telomerase holoenzyme, a complex
33 containing the telomerase reverse transcriptase (Trt1 in the fission yeast *Schizosaccharomyces*
34 *pombe*), an RNA template (TER1 in *S. pombe*), and accessory proteins that promote complex
35 assembly and tethering to telomeric DNA [1–4]. While the reverse transcriptase/RNA template
36 core of telomerase is generally well-conserved among eukaryotes, major differences exist,
37 including in the sequence and structure of the RNA template. In contrast to ciliate telomerase
38 RNAs, which are small RNA Polymerase III transcripts [5], yeast and metazoan telomerase RNAs
39 are longer and transcribed by RNA Polymerase II as precursors. These precursors then undergo
40 an extensive maturation process to yield the mature form that integrates into the telomerase
41 holoenzyme [3,4,6,7].
42
43 In *S. pombe,* the mature form of TER1 is generated from an intron-containing precursor through
44 a spliceosome-catalyzed reaction involving release of the 5' exon prior to exon ligation [8]. TER1
45 maturation then proceeds with the sequential binding of the Sm and Lsm complexes. Sm

46 proteins, well-characterized for their role in splicing, bind TER1 immediately upstream the 5'
47 splice site and promote 3' maturation and the addition of a 5' trimethylguanosine (TMG) cap by
48 the methyltransferase Tgs1 [9]. The Sm complex is then replaced by the Lsm2-8 complex, which
49 serves to protect the mature 3' end of TER1 from exonucleolytic degradation and promotes the
50 interaction between TER1 and Trt1 in the active telomerase holoenzyme. The switch from the
51 Sm to Lsm complexes correlates with distinct, non-overlapping substrates: TER1 precursors are
52 exclusively bound by the Sm complex, while the mature form of TER1, ending in a polyuridylate
53 stretch upstream the spliceosomal cleavage site, is only bound by the Lsm2-8 complex [9].
54
55 More recently, a role has been proposed for Pof8, a La-related protein 7 (LARP7) homolog, in
56 telomerase assembly and telomere maintenance in *S. pombe*. Ciliate LARP7 family proteins,
57 including p65 from *Tetrahymena thermophila*, have previously been characterized for their
58 functions in telomerase assembly [10]. Binding of p65 to stem IV of the *T. thermophila* telomerase
59 RNA TER results in a conformational change to the RNA and subsequent binding of the reverse
60 transcriptase TERT, suggesting a p65-dependent hierarchical assembly of the telomerase
61 holoenzyme [11]. Pof8 is hypothesized to function similarly in *S. pombe*, with Pof8 binding to TER1
62 promoting recruitment of the Lsm2-8 complex and enhancing the interaction between TER1
63 and Trt1. Accordingly, Pof8 deletion strains possess shorter telomeres indicative of a defect in
64 telomerase function [12–14]. Pof8 also functions in telomerase RNA quality control through
65 recognition of the correctly folded pseudoknot region and subsequent recruitment of the Lsm2-
66 8 complex to protect the 3' end from degradation [15]. Telomerase-related functions in LARP7
67 family proteins, particularly Pof8, map to a conserved C-terminal domain characteristic of

68 LARP7 family members, the extended RNA recognition motif (xRRM). The Pof8 xRRM is a major
69 determinant for Pof8-mediated telomerase activity, contributing to TER1 binding and complex
70 assembly [13,16]. As other fungal Pof8 homologs also possess an xRRM, it is anticipated that Pof8
71 may have a conserved role in telomere maintenance beyond fission yeast [13,17].
72
73 Conversely, LARP7 homologs in higher eukaryotes are best characterized in the transcriptional
74 regulatory 7SK snRNP, which includes the RNA polymerase III transcribed 7SK snRNA, the
75 methyl phosphate capping enzyme (MePCE), and hexamethylene bisacetamide-inducible
76 protein (HEXIM1/2). The 7SK snRNP inhibits transcription by sequestering positive transcription
77 elongation factor (P-TEFb) and preventing it from phosphorylating the C-terminal domain of the
78 largest subunit of RNA Polymerase II, which is associated with the transition into productive
79 transcription elongation [18–20]. The La module and xRRM of LARP7 bind 7SK through its
80 polyuridylate trailer and the 3' hairpin, respectively, and promote MePCE recruitment to the
81 complex [21,22]. In addition to adding a γ-monomethyl phosphate cap (i.e. CH_3-pppN) to 7SK
82 snRNA as a means of protecting it from 5' exonucleolytic degradation, MePCE remains stably
83 bound to 7SK snRNA to stabilize the complex [21]. MePCE, a homolog of the *Drosophila*
84 *melanogaster* Bin3/BCDIN3 protein, also catalyzes the addition of this atypical cap structure to
85 U6 snRNA [23]. Bin3/MePCE homologs are present in many eukaryotes, but to date little has been
86 studied outside of humans and *Drosophila* [24]. More recent work has identified BCIND3D, a
87 related Bin3 family protein overexpressed in breast cancer cells, as the enzyme responsible for
88 methylating the 5' monophosphate of histidine transfer RNA and pre-miR-145 [25,26]. Despite the

89 many insights into the role of Bin3/MePCE in RNA processing in higher eukaryotes, the function
90 of the essential *S. pombe* Bin3 homolog has yet to be determined [27,28].
91
92 In this work, we have explored the RNA targets of the *S. pombe* Bin3 homolog in an effort to
93 uncover its function. In addition to an expected association of Bin3 with the U6 snRNA, we
94 present data showing that Bin3 is a stable component of the *S. pombe* telomerase RNP. Our
95 results also provide evidence for an evolutionarily conserved interaction between Bin3 and
96 LARP7 homologs. Importantly, we show that the Bin3-Pof8 interaction is required for the
97 recruitment of Bin3 to both the U6 snRNA and the active telomerase holoenzyme. Additionally,
98 we provide evidence that Bin3 does not catalyze the addition of a γ-monomethyl phosphate
99 cap on TER1, suggesting a catalytic independent function. Rather, we present evidence that
100 Bin3 may negatively regulate telomerase activity, as decreased Bin3 expression correlates with
101 increases in steady-state levels of TER1 and longer telomeres. Taken together, our results
102 identify Bin3 as a novel component of the *S. pombe* telomerase holoenzyme, thus adding a new
103 layer of complexity to telomerase assembly and telomere maintenance.
104
105 **Results:**
106 ***S. pombe* Bin3 is essential and interacts with the U6 snRNA and the telomerase RNA TER1**
107 While Bin3/MePCE is conserved in many eukaryotes, its presence in the fission yeast *S. pombe*,
108 an organism lacking 7SK snRNA [24,29], is not well understood. Unlike the longer Bin3/MePCE
109 homologs from higher eukaryotes, *S. pombe* Bin3 only contains a conserved
110 methyltransferase/SAM-binding domain. Alignment of the methyltransferase domain of *S.*

111 *pombe* Bin3 to that of *H. sapiens* MePCE and *D. melanogaster* Bin3 reveals that previously
112 identified residues critical for SAM and SAH binding and nucleotide binding [30] are highly
113 conserved in *S.* pombe (Figure S1A,B). To validate genome-wide deletion screens identifying
114 Bin3 as an essential fission yeast protein [27,28], we ectopically expressed GST-tagged Bin3 cDNA
115 on the thiamine repressible pRep4x plasmid in a wild type strain and subsequently knocked out
116 the chromosomal copy (Figure S1C). Counter-selection of the Bin3-expressing plasmid on 5'FOA
117 resulted in lethality of the *bin3Δ* strain, with no phenotype for a wild type strain, confirming its
118 essential nature. Furthermore, overexpression of GST-Bin3 in wild-type *or bin3Δ* cells (i.e. in the
119 absence of thiamine) resulted in very slow growth, compared to normal growth when GST-Bin3
120 expression was repressed by addition of thiamine. Growth in the absence or presence of added
121 thiamine had no effect on cells transformed with an empty vector (Figure S1D). These data
122 thus suggest that in addition to Bin3 being essential, its overexpression is poorly tolerated in *S.*
123 *pombe*.
124
125 We next sought to determine the RNA substrates of *S. pombe* Bin3 to better understand its role
126 in the processing of fission yeast non-coding RNA(s). Following integration of a protein A (PrA)
127 tag into the Bin3 genomic locus, we performed RIP-Seq and plotted Bin3 IP reads against the IP
128 from an untagged strain, followed by validation of potential candidate substrates with northern
129 blotting (Figure 1, S2, Table S1). Consistent with previous reports of MePCE interacting with U6
130 snRNA [23], U6 emerged as one of the most highly enriched Bin3-interacting RNA transcripts. *S.*
131 *pombe* U6 is an unusual transcript in that it is transcribed by RNA Polymerase III yet contains an
132 mRNA-type intron removed by the spliceosome [31,32]. Alignment of RIP-Seq reads to the *S.*

133 *pombe* genome suggested that Bin3 interacts exclusively with the spliced form of U6. We
134 confirmed this with northern blotting, demonstrating robust immunoprecipitation of mature
135 U6 and no immunoprecipitation of the intron-containing precursor (Figure 1B). Chromatin
136 immunoprecipitation studies suggest that 7SK and U6 snRNA may be co-transcriptionally
137 modified by the human MePCE homolog [33], however our data are consistent with a model
138 wherein *S. pombe* Bin3 interacts with U6 post-splicing.
139
140 Surprisingly, the *S. pombe* telomerase RNA TER1 was also highly enriched in Bin3
141 immunoprecipitates (Figure 1A, C). Given the previously established link between the human
142 Bin3 homolog MePCE and human LARP7, [20] as well as the established link between the *S.*
143 *pombe* LARP7 homolog Pof8 and the telomerase holoenzyme [12–14], we considered the
144 possibility that Bin3 may also be part of the telomerase holoenzyme through an evolutionarily
145 conserved interaction with LARP7 family members.
146
147 **Bin3 interacts with the mature form of TER1**
148
149 Since TER1 processing and maturation involves a spliceosome-catalyzed reaction [8], we first set
150 out to determine the processing state of Bin3-associated TER1 by sequencing the 5' and 3' ends
151 through circularized rapid amplification of cDNA ends (Figure 2A). We also performed cRACE on
152 TER1 immunoprecipitated by Pof8, the telomerase reverse transcriptase Trt1, and Lsm3, all
153 known components of the mature TER1-containing active telomerase holoenzyme [3,4,9,12–14]. All
154 sequenced candidates had a discrete 5' end consistent with the reported 5' end [3,4] and a similar

155 distribution of 3' ends ending immediately upstream the 5' splice site [8], suggesting that Bin3
156 interacts with the full-length, 3' end-matured TER1 associated with the active telomerase
157 holoenzyme. The heterogeneity observed at the 3' end of all candidates is likely the result of
158 exonucleolytic nibbling prior to binding of the Lsm2-8 complex [9]. To investigate this further, we
159 subjected TER1 RNA immunoprecipitated by Bin3, Trt1, Pof8 and Lsm3 to RNase H cleavage to
160 generate shorter 5' and 3' fragments and compared fragment size by northern blot (Figure 2B).
161 The sizes of the 5' and 3' ends of TER1 were similar across immunoprecipitates, further
162 substantiating that Bin3 binds the mature form of TER1, rather than the intron-containing
163 precursor.
164
165 Further TER1 processing in *S. pombe* involves the addition of a 5' trimethylguanosine (TMG) cap
166 by Tgs1 [9]. Since Bin3 homologs are normally associated with the formation of a γ-monomethyl
167 phosphate cap, and to further understand when Bin3 interacts with TER1 with respect to TER1
168 processing, we examined the cap structure of Bin3-associated TER1 by immunoprecipitating
169 RNA associated with Bin3 and subsequently re-immunoprecipitating this RNA with an anti-TMG
170 antibody. The specificity of the anti-TMG antibody was confirmed by showing that it effectively
171 enriched the TMG cap containing U5 snRNA over the TMG cap lacking U6 snRNA or an
172 unrelated tRNA (Figure 2C). While Bin3-associated U6 snRNA was not immunoprecipitated by
173 the anti-TMG antibody, in agreement with data demonstrating the presence of a γ-monomethyl
174 phosphate cap [34], Bin3-associated TER1 RNA was effectively enriched by anti-TMG
175 immunoprecipitation. These data are consistent with previous work demonstrating a TMG cap
176 on TER1 in *S. pombe,* and also with Bin3 associating with TER1 following spliceosomeal cleavage

177 and 5' TMG capping, similar to what has been posited for Pof8 [12]. This suggests that Bin3
178 interacts with the primary cohort of TER1 transcripts, and not a γ-monomethyl phosphate
179 capped subset, and that TER1 is not a substrate for Bin3-catalyzed modification.
180
181 **Bin3 interacts with components of the mature telomerase holoenzyme**
182 Since our results indicate that Bin3 interacts with the mature form of TER1, we set out to
183 confirm the presence of Bin3 in the mature *S. pombe* telomerase holoenzyme. We
184 immunoprecipitated Bin3 and identified interacting proteins through mass spectrometry,
185 followed by validation using co-immunoprecipitation (Figure 3). We identified Pof8, the Lsm2-8
186 complex, and Trt1 in Bin3 immunoprecipitates, all of which make up the catalytically active core
187 telomerase holoenzyme [9,12–14,35–37] (Table S2, S3). We also detected the RNase P and RNase
188 MRP subunit Pop100 in Bin3 immunoprecipitations. Pop1, Pop6, and Pop7, subunits of RNase P
189 and RNase MRP in budding yeast, have recently been identified as components of the budding
190 yeast telomerase complex [38–40], suggesting that the involvement of RNase P and RNase MRP
191 subunits in telomere maintenance is evolutionarily conserved. The finding that Bin3 interacts
192 with core components of the telomerase holoenzyme, and not the Sm complex nor the TMG
193 capping enzyme Tgs1, suggests Bin3 does indeed associate with the active telomerase
194 holoenzyme rather than a precursor. The involvement of Bin3 in the telomerase holoenzyme
195 was further substantiated by gene ontology analysis to determine overrepresented biological
196 processes and cellular components among the top 50 Bin3 interactors. Telomerase holoenzyme
197 complex assembly and telomere maintenance via telomerase emerged as the top
198 overrepresented biological processes (Figure 3A). Similarly, overrepresented cellular

199 components include the Lsm2-8 complex, the telomerase holoenzyme, and spliceosomal
200 snRNPs (Table S4). We also repeated immunoprecipitations in the presence of benzonase to
201 determine if these interactions are direct or mediated through a nucleic acid intermediate
202 (Table S2). With the exception of Pof8, interactions between Bin3 and other components of the
203 telomerase holoenzyme were lost, indicative of an interaction mediated by TER1.
204
205 We confirmed the interactions between Bin3 and Pof8, as well as Bin3 and Trt1, through co-
206 immunoprecipitation (Figures 3B, 3C, S3). We also performed co-immunoprecipitations with
207 benzonase, demonstrating that the interaction between Bin3 and Pof8 persists with benzonase
208 treatment, while the Bin3-Trt1 interaction is lost (Figures 3B and 3C). The apparent nucleic acid-
209 dependence of the interaction between Bin3 and the majority of the telomerase holoenzymes
210 is reminiscent both of the budding yeast telomerase RNA TLC1, which acts as a scaffold to
211 nucleate telomerase holoenzyme assembly [41], as well as the MePCE/Bin3-containing 7SK snRNP
212 [42]. The finding that Bin3 and Pof8 interact directly is in agreement with previous reports
213 demonstrating a protein-protein interaction between MePCE and LARP7 in the context of the
214 vertebrate 7SK snRNP [33,42], suggesting the direct interaction may be evolutionarily conserved.
215
216 The apparent immunodepletion of Trt1 during Bin3 immunoprecipitation (Figure 3C, see
217 flowthrough lanes) indicated an absence of detectable Trt1-containing telomerase
218 holoenzymes lacking Bin3, substantiating the idea that Bin3 is a stoichiometric component of
219 the *S. pombe* telomerase holoenzyme. Consistent with this, benzonase treatment prior to Bin3
220 immunoprecipitation resulted in reappearance of Trt1 in the immunoprecipitation flowthrough.

221 On the other hand, affinity purification of Bin3 did not completely deplete Pof8 from the Bin3
222 immunoprecipitation flow through, consistent with either Bin3-independent functions for Pof8
223 or with possible dissociation of Pof8 from some Bin3-containing complexes (see U6, below)
224 (Figure 3B).
225
226 **Bin3 is recruited to the active telomerase holoenzyme through the LARP7 family protein Pof8**
227 We then tested whether Bin3 was recruited to the telomerase holoenzyme through its
228 interaction with Pof8, much like the human LARP7 homolog promotes MePCE recruitment to
229 7SK snRNA [21]. Immunoprecipitation of Bin3 in the context of a *pof8Δ* strain resulted in a
230 complete loss of TER1 binding, providing evidence that the interaction between Bin3 and TER1
231 is dependent on an interaction between Bin3 and Pof8 and Pof8 and TER1 (Figure 4A).
232 Unexpectedly, the interaction between Bin3 and U6 was also lost in the *pof8Δ.* Recent findings
233 indicate that human LARP7 binds U6 to guide post-transcriptional modification [43,44], so it is
234 tempting to speculate that Pof8 may also mediate Bin3 binding to U6 in fission yeast. To
235 address this, we immunoprecipitated Pof8 alongside Bin3 and other components of the
236 telomerase holoenzyme and looked for U6 enrichment. We observed slight enrichment of U6 in
237 Pof8-myc immunoprecipitates relative to immunoprecipitation using an untagged strain or the
238 Trt1-myc tagged strain (Figure 4B). We did not see enrichment for the intron-containing
239 precursor, suggesting that like Bin3, Pof8 interacts with the spliced form of U6. The slight
240 enrichment of U6 with a Pof8 immunoprecipitation, compared to the more robust
241 immunoprecipitation seen with Bin3 and Lsm3, suggests that Pof8 may transiently bind U6,
242 perhaps serving to load Bin3 on U6. Since LARP7 binding has been reported to disrupt the

243 catalytic activity of MePCE [33], a transient Pof8-U6 interaction may be consistent with U6
244 receiving a γ-monomethyl phosphate cap, compared to TER1, where stable Pof8 binding may
245 prevent Bin3 catalytic activity.
246
247 Knowing that Bin3 interacts with TER1 and components of the telomerase holoenzyme, we next
248 set out to confirm whether Bin3 is part of the catalytically active telomerase holoenzyme. We
249 performed a previously described *in vitro* telomerase assay that relies on the presence of the
250 TER1- and Trt1-containing telomerase holoenzyme to extend an oligonucleotide resembling
251 telomeric DNA [12]. Bin3 immunoprecipitates extended the oligonucleotide in a similar or greater
252 manner to Trt1 and Pof8 immunoprecipitates, as well as showed the same loss of activity upon
253 RNase A treatment, supporting the idea that Bin3, much like Pof8, is a component of the active
254 telomerase holoenzyme (Figure 4C). Consistent with our previous results, we also observed a
255 loss of activity for Bin3 immunoprecipitated from a *pof8Δ* strain, providing another line of
256 evidence that Bin3 is recruited to the telomerase holoenzyme through Pof8. Since Trt1 is only
257 recruited to the telomerase holoenzyme following Pof8 and Lsm2-8 binding, coupled with the
258 idea that the assay relies on the presence of a reverse transcriptase, these results are
259 consistent with a model in which Bin3 is recruited to TER1 through its interaction with Pof8 and
260 remains bound through subsequent holoenzyme assembly and the catalytic cycle (Figure 4D).
261
262 Evidence that Pof8 is required for telomerase holoenzyme assembly and maintenance of
263 telomere length [12–14], as well as for Bin3 recruitment to telomerase, prompted the question of
264 whether we could rescue the short telomere phenotype of a *pof8Δ* strain by overexpressing

265 Bin3. Consistent with a model in which Bin3 only assembles with the active telomerase
266 holoenzyme through its interaction with Pof8, Bin3 overexpression in a *pof8Δ* strain was
267 insufficient to rescue telomere shortening and the resultant chromosome fusions occurring
268 after telomeres reach a critically short length [12] (Figure S4).
269
270 **Bin3 negatively regulates TER1 accumulation and telomere lengthening**
271 Following the finding that Bin3 is a component of the *S. pombe* telomerase holoenzyme, we
272 wondered at the function of Bin3, and how it might interface with the stabilization and complex
273 assembly roles previously described for Pof8 [12–15]. As Bin3 deletion is lethal and its
274 overexpression results in a slow growth phenotype (Figure S1D), we varied Bin3 expression by
275 expressing plasmid-encoded Bin3 under the *nmt1* promoter in *bin3Δ* cells grown in rich media
276 containing thiamine. Under these conditions, we determined that thiamine-repressed, plasmid
277 encoded Bin3 was expressed approximately two-fold lower than Bin3 endogenously expressed
278 from the genomic locus (Figure 5A). Surprisingly, considering Pof8's role in TER1 stabilization,
279 we found this lower expression of Bin3 relative to wild type cells resulted in increased steady-
280 state levels of TER1 (Figure 5B). To determine the effects of Bin3 depletion on telomere length,
281 we continually passaged *bin3Δ* strains in minimal media containing supplemented thiamine and
282 visualized telomeres by southern blotting (Figure 5C). We observed a small but noticeable
283 telomere lengthening relative to a wild type strain, as well as the disappearance of a lower
284 band. Taken together, our results suggest that Bin3 may act as a negative regulator to limit
285 TER1 levels and telomerase activity under wild type conditions, in contrast to the stabilizing
286 roles of its binding partner Pof8.

287

288 **Pof8-like proteins are associated with Bin3-like proteins in diverse fungal lineages**

289 The interaction between Bin3 and Pof8, coupled with the conservation of such an interaction in
290 other examined eukaryotes, led us to wonder at the extent of this interaction on a phylogenetic
291 scale. While Bin3/MePCE and LARP7/Pof8 family members are ubiquitous in higher eukaryotes,
292 their absence or presence is more varied in fungal lineages. We queried hundreds of
293 representative fungal species for the presence of Bin3- and Pof8-like proteins and identified
294 many species with a) both a Bin3 and Pof8 homolog, b) only a Bin3 homolog, or c) neither a
295 Bin3 nor a Pof8 homolog (Figure 6, S5). Conversely, only four out of 472 examined species
296 contained a Pof8-like protein but no Bin3-like protein, and in these species the Pof8 homolog
297 was noted to have a shortened N-terminal domain that would lack the La module observed in
298 other LARP7 family members, raising the possibility that members of this rare cohort may not
299 be bona-fide LARP7 family members, at least as these are currently appreciated [17]. Based on
300 the observed distribution, it seems likely that both genes were present in a fungi common
301 ancestor, but Pof8 or both Bin3 and Pof8 were lost in certain lineages. Examination of the
302 distribution of Bin3 and LARP7-family members in basal eukaryotic lineages reveals a similar
303 pattern: Bin3 can be present without LARP7, but there are no instances where a LARP7-family
304 member exists in a lineage lacking a Bin3 homolog (Table S9). Similarly, LARP7-family proteins
305 are represented in Alveolates, Stramenopiles, Amoebozoa, Fungi, and Metazoans, while Bin3-
306 family proteins are present in all eukaryotic lineages. Since the presence of Pof8/LARP7 is very
307 highly linked to the presence of a Bin3 homolog, these data suggest that the function of LARP7

308 family members may be more intimately associated with the function of Bin3/MePCE than has
309 been previously appreciated.
310
311 **Discussion:**
312 In this study, we have identified Bin3 as a novel component of the *S. pombe* telomerase
313 holoenzyme. In addition to showing an interaction between Bin3 and U6 snRNA, we
314 demonstrate that Bin3 interacts with the telomerase RNA TER1 and components of the active
315 telomerase holoenzyme in a manner that is dependent on the presence of the LARP7 family
316 protein Pof8. Together, our results indicating that Bin3 interacts with the mature, spliced form
317 of TER1 and Bin3 immunoprecipitates possess telomerase activity *in vitro* strongly suggest that
318 Bin3 is a constitutive component of the telomerase holoenzyme containing Trt1, Pof8, Lsm2-8,
319 and Est1 scaffolded on TER1 (Figure 4D). The idea of Pof8 and Bin3 scaffolded on TER1 is
320 reminiscent of LARP7 and MePCE in the 7SK snRNP, with Pof8/LARP7 recruiting Bin3/MePCE to
321 the RNA substrate. Similar to our data showing Pof8 recruiting Bin3 to TER1 and the telomerase
322 holoenzyme, LARP7 has also been demonstrated to recruit MePCE to the 7SK snRNP in human
323 cells [21]. Thus, the protein-protein interaction and subsequent recruitment to RNA substrates by
324 LARP7 appears evolutionarily conserved in fission yeast and higher eukaryotes. We also present
325 data demonstrating that the presence of Pof8-like proteins is nearly universally correlated with
326 the presence of Bin3-like proteins in fungi, suggesting that the Bin3-Pof8 interaction is highly
327 conserved and more prevalent than previously anticipated. Since Pof8 is required to load Bin3
328 onto the telomerase RNA and U6 snRNA in fission yeast, this phylogenetic distribution raises

329 the question of whether Bin3 homologs in fungi lacking a LARP7 homolog have evolved a
330 mechanism to bind RNA targets in a Pof8/LARP7 independent fashion.
331
332 Since TER1 undergoes several processing steps before assembly into the telomerase
333 holoenzyme, we were able to assess TER1 processing state to determine when Bin3 interacts
334 with TER1 with respect to the timing of TER1 maturation. We show that Bin3-associated TER1
335 has a mature 3' end, indicative of spliceosome-catalyzed end processing, and a 5' TMG cap. This
336 is consistent with previously reported data on the timing of Pof8 binding; since our data
337 indicates that the interaction between Bin3 and TER1 is dependent on Pof8, the most
338 parsimonious explanation is that Pof8, and thus Bin3, bind TER1 following 3' maturation and
339 TMG capping, preceding the binding of the Lsm2-8 complex [12]. We show that the interaction
340 between Bin3 and TER1 is dependent on Pof8, leading to the conclusion that Bin3 interacts with
341 TER1 at the same stage as Pof8, resulting in the hierarchical assembly of the active telomerase
342 holoenzyme.
343
344 The finding that Bin3-associated TER1 is immunoprecipitated by a TMG antibody argues against
345 a catalytic role for Bin3 in TER1 processing. Our data, coupled with previous work characterizing
346 the cap structure on the mature TER1 bound to Trt1 [3,4], supports the idea that Bin3 has a
347 capping-independent function in the telomerase holoenzyme. LARP7 binding to MePCE in the
348 7SK snRNP inhibits its capping activity; MePCE, in turn, promotes the interaction between 7SK
349 and LARP7, thereby stabilizing the complex [33]. In the *S. pombe* telomerase holoenzyme and U6
350 snRNP, we can hypothesize that Pof8 may also inhibit the methyltransferase activity of Bin3 by

351 binding to and obscuring the active site. This is consistent with our results suggesting a
352 transient interaction between Pof8 and U6 that may function to load Bin3 on U6. In such a
353 model, an interaction between Bin3 and Pof8 is necessary to recruit Bin3 to U6 and following
354 dissociation of Pof8, the catalytic site of Bin3 would become available to cap U6.
355
356 Additionally, our work identifying Bin3 as a telomerase-associated protein brings to mind work
357 identifying a box H/ACA motif at the 3' end of vertebrate telomerase RNA [45]. Box H/ACA RNAs
358 form an RNP complex with Dyskerin/Cbf5, Nop10, Nhp2, and Gar1 to guide noncoding RNA
359 pseudouridylation [46,47]. Although Dyskerin is a pseudouridine synthase, to date no evidence has
360 pointed to a modification function for Dyskerin in the context of telomerase RNA. Rather, the
361 Dyskerin-containing H/ACA complex has a structural role in telomerase biogenesis, with binding
362 of the H/ACA RNP to telomerase RNA leading to a conformational change in the RNA that
363 promotes 3' processing and maturation over exosome-mediated decay [48]. This is reminiscent of
364 the apparent catalytic independent role we observed for Bin3 in fission yeast telomerase,
365 although our data point towards Bin3 having a role in limiting TER1 accumulation, perhaps as a
366 negative regulator of telomere elongation.
367
368 Bin3 and Pof8 having seemingly opposing functions in TER1 maturation and the telomerase RNP
369 may provide an explanation as to the viability of Pof8 knockout strains, while Bin3 knockouts
370 are lethal. Assuming Bin3 functions in limiting telomerase activity by decreasing TER1 levels, a
371 lack of Bin3 negative regulation may be detrimental, much like the shelterin component Tpz1
372 and the telomere cap complex subunit Stn1, both of which are negative regulators of

373 telomerase and essential proteins in *S. pombe* [27,49]. In contrast, since Pof8 promotes telomerase
374 activity, its deletion doesn't result in unchecked telomere lengthening. It remains to be found
375 how exactly Bin3 limits TER1 accumulation but it is possible that Bin3 interfaces with decay
376 pathways, such as the established exosome-mediated 3' decay pathway [12,14] or an as yet
377 undiscovered pathway analogous to the 5' decay of human telomerase RNA [50]. Bin3 may
378 therefore be important for maintaining telomere homeostasis by decreasing TER1 levels under
379 conditions where cell cycle progression or telomere lengthening are unfavorable.
380
381 Another facet of this work builds on the idea that components of the telomerase holoenzyme
382 are more conserved than previously appreciated. In addition to the ubiquitous telomerase
383 reverse transcriptase, previous work has identified LARP7 family proteins in both ciliates and
384 yeast [10,12–14], arguing a level of evolutionary conservation. Other recent findings implicate the
385 human LARP7 homolog in telomere maintenance [51], suggesting this conservation may extend to
386 higher eukaryotes. We now also provide evidence indicating the presence of RNase P and
387 RNase MRP subunits in fission yeast, much like the RNase P and RNase MRP subunits found in
388 the budding yeast telomerase complex [38–40]. The presence of RNase P and RNase MRP subunits
389 in two divergent yeast species supports the importance of these factors in the function of a
390 breadth of telomerase holoenzymes.
391
392 Our results indicating that Bin3 is part of the telomerase holoenzyme were quite unexpected,
393 as Bin3 has been well-characterized in higher eukaryotes for its role in the processing,
394 maturation, and protection of RNA Polymerase III transcripts [23,33]. An intriguing idea involves

395 polymerase switching through telomerase RNA evolution. Ciliate telomerase RNA is transcribed
396 by RNA Polymerase III and subsequently binds the LARP7 homolog p65 through the terminal
397 polyuridylate stretch common to RNA Polymerase III transcripts [10,52]. Since MePCE and LARP7
398 also associate with RNA Polymerase III transcripts, it is possible that the Pof8-bound RNA
399 Polymerase II transcribed TER1, and the *S. pombe* telomerase RNP as a whole, represent an
400 intermediate step in the evolution of telomerase RNA between ciliates and the RNA Polymerase
401 II transcribed telomerase RNA of higher eukaryotes. Future work should investigate the
402 presence of Bin3/MePCE homologs in the telomerase holoenzymes of other species,
403 particularly in ciliates, which possess both an RNA Polymerase III transcribed telomerase RNA
404 and a LARP7 homolog. Such findings will continue to develop emerging ideas regarding
405 conservation in telomerase RNA processing and the composition of telomerase RNPs.
406

407 **Acknowledgements:**
408 We thank Toru Nakamura and Virginia Zakian for sharing published yeast strains and Marc
409 Fabian and Raymund Wellinger for helpful comments on the manuscript. J.P. is supported by a
410 Canada Graduate Scholarship (Doctoral) from the National Sciences and Engineering Research
411 Council of Canada. M.A.B. is supported by a Discovery Grant from NSERC ("Impact of chemical
412 modification of non-coding RNAs on gene expression in *S. pombe*"). JMD is supported by the
413 Institut Universitaire de France (IUF), JMD and MEB by the CNRS and the University of
414 Perpignan (UPVD) and their study is set within the framework of the "Laboratoires
415 d'Excellences (LABEX)" TULIP (ANR-10-LABX-41) and of the "École Universitaire de Recherche
416 (EUR)" TULIP-GS (ANR-18-EURE-0019).

417

418

419 **Author contributions:**

420 J.P. conceived of the study, designed, performed, and analyzed all experiments, and wrote the

421 first draft of the manuscript with input from all authors. M.E.B. and J-M.D. performed

422 phylogenetic analysis. J.G. and J.P. analyzed RNA-Seq data. M.A.B. conceived of the study,

423 designed experiments, supervised the project, and edited the manuscript.

424

425 **Materials and Methods:**

426 Strains, constructs, and growth media

427 Strains were grown in yeast extract with supplements (YES) or Edinburgh Minimal Media

428 (EMM), as indicated. Expression of genes under the control of the *nmt1* promoter was

429 repressed with the addition of 15 μM thiamine. Tag integration and knockouts were generated

430 with a previously described PCR-based strategy and verified by PCR and western blotting [53]

431 (primer sequences in Table S6). Protein A-tagged strains were generated according to [54].

432 Correct genotypes were selected on YES plates with the corresponding antibiotic (200 μg/mL

433 G418, Sigma; 100 μg/mL Nourseothricin, GoldBio; 100 μg/mL phleomycin, Invivogen). Other

434 strains were created by mating and antibiotic selection. A list of strains is provided in Table S5.

435

436 Native protein extract and immunoprecipitation

437 *S. pombe* cells were grown in YES at 30°C to mid-log phase, harvested, and subject to cryogenic

438 disruption using a mortar and pestle. Cell powder was lysed in 50 mM NaCl, 20 mM Hepes pH

439 7.4, 55 mM KOAc, 0.5% Triton X, 0.1% Tween-20, 0.2 mM PMSF, 1:100 Protease Inhibitor
440 Cocktail (Thermo, 78430), and 0.004 U/μL RNase inhibitor (Invitrogen, AM2694). For Protein A-
441 tagged strains, immunoprecipitation was carried out with Rabbit IgG-conjugated (MP-
442 Biomedicals, SKU 085594) Dynabeads (Invitrogen, 14301) as described [55]. Myc-tagged proteins
443 were immunoprecipitated with Protein G Dynabeads (Invitrogen, 10003D) coated with anti-myc
444 antibody (Sigma, M4439). Beads were washed 4 times with 400 μL lysis buffer. For RNA
445 immunoprecipitations, bound RNA was isolated by treatment of beads with 0.1% SDS and 0.2
446 mg/mL Proteinase K (Sigma, P2308) at 37°C for 30 minutes, followed by extraction with phenol:
447 chloroform:isoamyl alcohol (25:24:1) and ethanol precipitation.
448
449 RNA preparation and Northern blotting
450 Total RNA was isolated from native protein extracts by incubation with 0.5% SDS, 0.2 mg/mL
451 proteinase K (Sigma, P2308), 20 mM Tris HCl pH 7.4, and 10 mM EDTA pH 8.0 for 15 minutes at
452 50°C, followed by phenol: chloroform extraction and ethanol precipitation. Northern blot
453 analysis was performed as described using 8% TBE-urea polyacrylamide gels [56]. Briefly,
454 electrophoresed RNA was transferred to positively charged nylon membranes (Perkin Elmer,
455 NEF988001) with the iBlot 2 system (Thermo, IB21001) and probed with ^{32}P γ-ATP-labeled DNA
456 probes (probe sequences provided in Table S7). For RNase H digestion, RNA was incubated with
457 25 pmol RNase H probe (provided in Table S7) for 5 minutes at 65°C and slow cooled to 37°C,
458 followed by digestion with 5 U RNase H (NEB, M02975) for 30 minutes at 37°C. The reaction
459 was stopped with the addition of 25 μM EDTA pH 8.0 and phenol: chloroform extraction and

460 ethanol precipitation. TMG-capped RNAs were isolated from RNase H-treated

461 immunoprecipitates with an α-TMG agarose conjugate (Sigma, NA02A), according to [4].

462

463 qRT-PCR

464 1 μg Turbo DNase-treated RNA was reverse transcribed with the iScript cDNA synthesis kit

465 (BioRad, 1708890), treated with 0.5 μL RNase cocktail (Invitrogen, AM2286), and diluted 1:10.

466 cDNA was quantified using the SensiFAST SYBR No-Rox kit (Bioline, BIO-98005) and 1 μM of

467 each primer (primer sequences provided in Table S7). qPCR settings were as follows: 95°C for

468 10 minutes and 40 cycles consisting of 10 seconds at 95°C, 20 seconds at 60°C, and 20 seconds

469 at 72°C, followed by melting curve analysis. *Bin3 mRNA* levels were normalized to *his1 mRNA*

470 levels and subsequently subject to paired two-tailed student's *t*-tests (n=3 biological replicates,

471 each with 6 technical replicates).

472

473 RNA Seq and RIP Seq

474 Libraries were constructed from immunoprecipitated RNA samples and rRNA-depleted total

475 RNA samples by the TCAC Sequencing Facility at the Hospital for Sick Children in Toronto.

476 Libraries were sequenced on an Illumina Hi-Seq 2500 for 50-bp single-end reads. Reads were

477 mapped to the *S. pombe* ASM294v2 genome using kallisto [57] using parameters –single –

478 fragment-length=50 –sd=5 and subsequently visualized on IGV [58]. Reads were filtered to

479 include transcripts containing 4 or more reads in at least one of the Bin3 immunoprecipitated

480 replicates and TPM values were subject to median-normalization. Gaussian mixture modeling

481 (GMM) was applied to calculate the probability of an interaction using log of odds [59]. Reads

482 were further filtered to exclude transcripts with a log of odds score less than 3.17. The log of
483 the average of median-normalized TPM values from the Bin3 immunoprecipitates was plotted
484 against that of the control immunoprecipitations.
485
486 Circularized Rapid Amplification of cDNA Ends (cRACE)
487 Immunoprecipitated RNA was treated with 2 U TURBO DNase (Invitrogen, AM2239) and
488 dephosphorylated with 1 U calf intestinal alkaline phosphatase (NEB, M0290), followed by
489 decapping and circularization with RNA 5' Pyrophosphohydrolase (NEB, M0356S) and T4 RNA
490 Ligase 1 (NEB, M0204S). TER1 was amplified from circularized RNA with the OneStep RT-PCR Kit
491 (Qiagen, 210210) (primer sequences in Table S7). cRACE products were cloned into the pGEM-T
492 vector (Promega, A1360) and sequenced by the TCAG DNA Sequencing Facility at the Hospital
493 for Sick Children in Toronto.
494
495 Mass spectrometry and GO analysis
496 Half of the native protein extract was pre-treated with 0.625 U/μL Benzonase (Millipore, E1014)
497 at 37°C for 30 minutes. The reaction was stopped with 5 mM EDTA pH 8.0 and Protein A
498 immunoprecipitation was performed in the same manner as for RNA immunoprecipitations.
499 After washes with lysis buffer, beads were washed with 0.1 M NH_4OAc and 0.1 mM $MgCl_2$ and
500 eluted with 0.5 M NH_4OH for 20 minutes at room temperature. Eluates were lyophilized and
501 subject to in-solution tryptic digestion. LC-MS/MS analysis was performed by the IRCM
502 Proteomics Discovery Platform on a Q Exactive HF.
503

504 Raw data was processed and analyzed using the MaxQuant software package 1.5.1.2 [60] and the
505 fission yeast UP000002485 reference proteome (24/11/2019). Settings used for MaxQuant
506 analysis were as reported [61]. Proteins present in immunoprecipitations from both biological
507 replicates and absent from control immunoprecipitations were considered genuine Bin3
508 interacting partners and ranked by peak intensity. PANTHER overrepresentation tests (GO
509 Ontology database released 2019-12-09) were conducted on the top 50 Bin3 interacting
510 partners. Fisher's exact tests with FDR correction were performed using the GO biological
511 process complete and GO cellular component complete data sets.
512
513 Co-immunoprecipitation and western blotting
514 Cells were harvested at mid-log phase, resuspended in lysis buffer (10 mM Tris HCl pH 7.5, 150
515 mM NaCl, 0.5% NP40, 1:100 Protease Inhibitor Cocktail), and lysed with acid-washed glass
516 beads (Sigma, G8772). Immunoprecipitations were carried out as described and proteins were
517 eluted by resuspending beads in 2X SDS loading buffer (100 mM Tris HCl pH 6.8, 4% SDS, 20%
518 glycerol, 0.2% bromophenol blue) and boiling at 95°C for 5 minutes. Western blot analyses
519 were performed using monoclonal anti-myc (Cell Signaling, 2276S) at 1:5000 and monoclonal
520 anti-beta actin (abcam, ab8226) at 1:2500 for primary antibodies and HRP-conjugated anti-
521 mouse at 1:5000 for secondary antibodies. Protein A-tagged proteins were detected with HRP-
522 conjugated polyclonal anti-Protein A (Invitrogen, PA1-26853) at 1:5000.
523
524 Telomerase activity assay

525 The telomerase activity assay was performed as described [12]. Briefly, bead slurries (see
526 immunoprecipitation) were incubated at 30°C for 90 minutes in a 10 μL reaction containing 50
527 mM Tris HCl pH 8.0, 1 mM MgOAc, 5% glycerol, 1 mM spermidine, 1 mM DTT, 100 mM KOAc,
528 0.2 mM dATP, dCTP, and dTTP, 5 μM telomerase assay primer (Table S7), and 0.3 μM 3000
529 Ci/mmol [α-^{32}P] dGTP (Perkin Elmer, BLU512H250UC). The reaction was stopped with the
530 addition of 0.5% SDS, 10 mM EDTA pH 8.0, 20 mM Tris HCl pH 7.5, 2 μg/μL Proteinase K
531 (Sigma), and 10000 cpm [γ-^{32}P] ATP-labeled 100-mer oligonucleotide and incubation at 42°C for
532 15 minutes, followed by phenol: chloroform extraction and ethanol precipitation. RNase A-
533 treated samples were pre-incubated with 20 ng RNase A (Invitrogen, AM2271) at 30°C for 10
534 minutes. Extension products were separated on a 10% urea-TBE polyacrylamide sequencing gel
535 at 60 W for 90 minutes, dried and exposed to a PhosphorScreen, and imaged with a Typhoon
536 imager.
537
538 Genomic DNA extraction, southern blotting, and chromosome fusion PCR
539 Genomic DNA was extracted from logarithmically growing cells according to [13]. For southern
540 blotting, 15 μg genomic DNA was digested overnight with EcoRI and separated on a 1% agarose
541 gel, transferred to positively charged nylon membranes (Perkin Elmer, NEF988001) by capillary
542 transfer in 10X SSC, and probed with a ^{32}P γ-ATP-labeled telomere probe (probe sequence
543 provided in Table S7). The chromosome fusion PCR was adapted from [12]. Briefly, 50 μL PCR
544 reactions contained 1 μL genomic DNA, 0.4 μM forward and reverse primers (sequences
545 provided in Table S7), 200 μM dNTPs, 1X Taq ThermoPol Buffer (NEB), and 1.25 U Taq
546 Polymerase (NEB, M0273). The Trt1 gene was amplified as a loading control in an identical PCR

547 reaction containing the corresponding primers. The PCR reaction consisted of an initial
548 denaturation at 95°C for 5 minutes, followed by 32 cycles of 95°C for 15 seconds, 55°C for 30
549 seconds, and 68°C for 3 minutes, with a final extension at 68°C for 10 minutes.
550
551 Structure prediction
552 The structure of *S. pombe* Bin3 was predicted using Phyre2 [62] and aligned with the co-crystal
553 structure of the *H. sapiens* MePCE methyltransferase domain bound to 7SK snRNA and SAH
554 (6DCB [30]) in PyMol [63]. Primary sequences were aligned with the Clustal Omega Multiple
555 Sequence Alignment tool [64].
556
557 Phylogenetic tree construction and search for Bin3-like and Pof8-like sequences
558 Protein sequences (GeneCatalogs) of 472 fungal species were downloaded from the JGI website
559 (https://mycocosm.jgi.doe.gov/) in fasta format. 5614520 proteins were downloaded and
560 merged into a single multifasta file. A blast (Blastp) against all proteins was performed using
561 diamond blastp [65] with a minimum e-value of 1e-5 and outfmt 6 (for tabular output). In order to
562 identify homologous proteins, proteins were clustered together if they shared at least 50%
563 similarity over 70% of coverage using SiLiX [66]. When a cluster contained two or more paralogous
564 genes derived from duplications, the species was removed from the cluster. Finally, only
565 clusters with a minimum of 100 species were retained for further analysis. Following these
566 cleaning steps, we obtained 5328 clusters containing one gene per species. Proteins sequences
567 of each cluster were aligned using MAFFT (v7.271) with default parameters
568 (https://mafft.cbrc.jp/alignment/server/). Multiple alignments were cleaned using trimA1

569 (v1.4.rev22 build [2015-05-21]) with -st 0.01 option. Fastree (version 2.1.10 SSE3) with default
570 parameters were used to build phylogenetic trees [67]. The consensus fungi tree was obtained
571 using ASTRAL (astral.5.6.3) software with default parameters [68]. To detect the presence of
572 genes coding for Bin3-like and Pof8-like proteins, blast searches (blastp and tbalstn) were
573 performed on each studied fungus genome, using initially either the full-length *S. pombe* Bin3
574 protein sequence or the *S. pombe* Pof8 xRRM conserved motif. This procedure was repeated in
575 each fungal clade using clade-specific Bin3-like and Pof8-like sequences detected by the initial
576 search using *S. pombe* sequences. Finally, new blast searches were performed all over again,
577 this time using Bin3-like or Pof8-like "probes" made of a collection of sequences representing
578 the diversity of these two proteins in fungi.
579
580 Data availability
581 Mass spectrometry proteomics and RNA Seq data will be supplied prior to publication.
582
583
584
585
586
587
588
589
590

591 **References:**

592 1. Collins, K. The biogenesis and regulation of telomerase holoenzymes. *Nature Reviews*
593 *Molecular Cell Biology* (2006) doi:10.1038/nrm1961.
594 2. Blackburn, E. H. & Collins, K. Telomerase: An RNP enzyme synthesizes DNA. *Cold Spring*
595 *Harb. Perspect. Biol.* (2011) doi:10.1101/cshperspect.a003558.
596 3. Leonardi, J., Box, J. A., Bunch, J. T. & Baumann, P. TER1, the RNA subunit of fission yeast
597 telomerase. *Nat. Struct. Mol. Biol.* (2008) doi:10.1038/nsmb1343.
598 4. Webb, C. J. & Zakian, V. A. Identification and characterization of the
599 Schizosaccharomyces pombe TER1 telomerase RNA. *Nat. Struct. Mol. Biol.* (2008)
600 doi:10.1038/nsmb1354.
601 5. Greider, C. W. & Blackburn, E. H. A telomeric sequence in the RNA of Tetrahymena
602 telomerase required for telomere repeat synthesis. *Nature* (1989)
603 doi:10.1038/337331a0.
604 6. Feng, J. *et al.* The RNA component of human telomerase. *Science (80-.).* (1995)
605 doi:10.1126/science.7544491.
606 7. Chapon, C., Cech, T. R. & Zaug, A. J. Polyadenylation of telomerase RNA in budding yeast.
607 *RNA* (1997).
608 8. Box, J. A., Bunch, J. T., Tang, W. & Baumann, P. Spliceosomal cleavage generates the 3'
609 end of telomerase RNA. *Nature* (2008) doi:10.1038/nature07584.
610 9. Tang, W., Kannan, R., Blanchette, M. & Baumann, P. Telomerase RNA biogenesis involves
611 sequential binding by Sm and Lsm complexes. *Nature* (2012) doi:10.1038/nature10924.
612 10. Witkin, K. L. & Collins, K. Holoenzyme proteins required for the physiological assembly

613 and activity of telomerase. *Genes Dev.* (2004) doi:10.1101/gad.1201704.

614 11. O'Connor, C. M. & Collins, K. A Novel RNA Binding Domain in Tetrahymena Telomerase
615 p65 Initiates Hierarchical Assembly of Telomerase Holoenzyme. *Mol. Cell. Biol.* (2006)
616 doi:10.1128/mcb.26.6.2029-2036.2006.

617 12. Páez-Moscoso, D. J. *et al.* Pof8 is a La-related protein and a constitutive component of
618 telomerase in fission yeast. *Nat. Commun.* (2018) doi:10.1038/s41467-017-02284-8.

619 13. Mennie, A. K., Moser, B. A. & Nakamura, T. M. LARP7-like protein Pof8 regulates
620 telomerase assembly and poly(A)+TERRA expression in fission yeast. *Nat. Commun.*
621 (2018) doi:10.1038/s41467-018-02874-0.

622 14. Collopy, L. C. *et al.* LARP7 family proteins have conserved function in telomerase
623 assembly. *Nat. Commun.* (2018) doi:10.1038/s41467-017-02296-4.

624 15. Hu, X. *et al.* Quality-Control Mechanism for Telomerase RNA Folding in the Cell. *Cell Rep.*
625 (2020) doi:10.1016/j.celrep.2020.108568.

626 16. Basu, R., Eichhorn, C. D., Cheng, R., Peterson, R. D. & Feigon, J. Structure of S. pombe
627 telomerase protein Pof8 C-terminal domain is an xRRM conserved among LARP7
628 proteins. *RNA Biol.* (2020) doi:10.1080/15476286.2020.1836891.

629 17. Deragon, J.-M. M. Distribution, organization an evolutionary history of La and LARPs in
630 eukaryotes. *RNA Biol.* 1–9 (2020) doi:10.1080/15476286.2020.1739930.

631 18. Nguyen, V. T., Kiss, T., Michels, A. A. & Bensaude, O. 7SK small nuclear RNA binds to and
632 inhibits the activity of CDK9/cyclin T complexes. *Nature* (2001) doi:10.1038/35104581.

633 19. Yang, Z., Zhu, Q., Luo, K. & Zhou, Q. The 7SK small nuclear RNA inhibits the CDK9/cyclin
634 T1 kinase to control transcription. *Nature* (2001) doi:10.1038/35104575.

635 20. Krueger, B. J. *et al.* LARP7 is a stable component of the 7SK snRNP while P-TEFb, HEXIM1
636 and hnRNP A1 are reversibly associated. *Nucleic Acids Res.* (2008)
637 doi:10.1093/nar/gkn061.
638 21. Muniz, L., Egloff, S. & Kiss, T. RNA elements directing in vivo assembly of the
639 7SK/MePCE/Larp7 transcriptional regulatory snRNP. *Nucleic Acids Res.* (2013)
640 doi:10.1093/nar/gkt159.
641 22. Eichhorn, C. D., Chug, R. & Feigon, J. hLARP7 C-terminal domain contains an xRRM that
642 binds the 3' hairpin of 7SK RNA. *Nucleic Acids Res.* (2016) doi:10.1093/nar/gkw833.
643 23. Jeronimo, C. *et al.* Systematic Analysis of the Protein Interaction Network for the Human
644 Transcription Machinery Reveals the Identity of the 7SK Capping Enzyme. *Mol. Cell*
645 (2007) doi:10.1016/j.molcel.2007.06.027.
646 24. Cosgrove, M. S., Ding, Y., Rennie, W. A., Lane, M. J. & Hanes, S. D. The bin3 RNA
647 methyltransferase targets 7SK RNA to control transcription and translation. *Wiley*
648 *Interdisciplinary Reviews: RNA* (2012) doi:10.1080/09540121.2017.1344767.
649 25. Xhemalce, B., Robson, S. C. & Kouzarides, T. Human RNA methyltransferase BCDIN3D
650 regulates MicroRNA processing. *Cell* (2012) doi:10.1016/j.cell.2012.08.041.
651 26. Martinez, A. *et al.* Human BCDIN3D monomethylates cytoplasmic histidine transfer RNA.
652 *Nucleic Acids Res.* (2017) doi:10.1093/nar/gkx051.
653 27. Kim, D. U. *et al.* Analysis of a genome-wide set of gene deletions in the fission yeast
654 Schizosaccharomyces pombe. *Nat. Biotechnol.* (2010) doi:10.1038/nbt.1628.
655 28. Hayles, J. *et al.* A genome-wide resource of cell cycle and cell shape genes of fission
656 yeast. *Open Biol.* (2013) doi:10.1098/rsob.130053.

657 29. Marz, M. *et al.* Evolution of 7SK RNA and its protein partners in metazoa. *Mol. Biol. Evol.*
658 (2009) doi:10.1093/molbev/msp198.
659 30. Yang, Y., Eichhorn, C. D., Wang, Y., Cascio, D. & Feigon, J. Structural basis of 7SK RNA 5'-γ-
660 phosphate methylation and retention by MePCE. *Nat. Chem. Biol.* (2019)
661 doi:10.1038/s41589-018-0188-z.
662 31. Tani, T. & Ohshima, Y. The gene for the U6 small nuclear RNA in fission yeast has an
663 intron. *Nature* (1989) doi:10.1038/337087a0.
664 32. Tani, T. & Ohshima, Y. mRNA-type introns in U6 small nuclear RNA genes: Implications for
665 the catalysis in pre-mRNA splicing. *Genes Dev.* (1991) doi:10.1101/gad.5.6.1022.
666 33. Xue, Y., Yang, Z., Chen, R. & Zhou, Q. A capping-independent function of MePCE in
667 stabilizing 7SK snRNA and facilitating the assembly of 7SK snRNP. *Nucleic Acids Res.*
668 (2009) doi:10.1093/nar/gkp977.
669 34. Gu, J., Patton, J. R., Shimba, S. & Reddy, R. Localization of modified nucleotides in
670 Schizosaccharomyces pombe spliceosomal small nuclear RNAs: Modified nucleotides are
671 clustered in functionally important regions. *RNA* (1996).
672 35. Nakamura, T. M. *et al.* Telomerase catalytic subunit homologs from fission yeast and
673 human. *Science (80-.).* (1997) doi:10.1126/science.277.5328.955.
674 36. Beernink, H. T. H., Miller, K., Deshpande, A., Bucher, P. & Cooper, J. P. Telomere
675 maintenance in fission yeast requires an est1 ortholog. *Curr. Biol.* (2003)
676 doi:10.1016/S0960-9822(03)00169-6.
677 37. Webb, C. J. & Zakian, V. A. Schizosaccharomyces pombe Ccq1 and TER1 bind the 14-3-3-
678 like domain of Est1, which promotes and stabilizes telomerase-telomere association.

679 *Genes Dev.* (2012) doi:10.1101/gad.181826.111.

680 38. Lemieux, B. *et al.* Active Yeast Telomerase Shares Subunits with Ribonucleoproteins
681 RNase P and RNase MRP. *Cell* (2016) doi:10.1016/j.cell.2016.04.018.

682 39. Garcia, P. D. *et al.* Stability and nuclear localization of yeast telomerase depend on
683 protein components of RNase P/MRP. *Nat. Commun.* (2020) doi:10.1038/s41467-020-
684 15875-9.

685 40. Lin, K. W. *et al.* Proteomics of yeast telomerase identified Cdc48-Npl4-Ufd1 and Ufd4 as
686 regulators of Est1 and telomere length. *Nat. Commun.* (2015) doi:10.1038/ncomms9290.

687 41. Zappulla, D. C. & Cech, T. R. Yeast telomerase RNA: A flexible scaffold for protein
688 subunits. *Proc. Natl. Acad. Sci. U. S. A.* (2004) doi:10.1073/pnas.0403641101.

689 42. Barboric, M. *et al.* 7SK snRNP/P-TEFb couples transcription elongation with alternative
690 splicing and is essential for vertebrate development. *Proc. Natl. Acad. Sci. U. S. A.* (2009)
691 doi:10.1073/pnas.0903188106.

692 43. Hasler, D. *et al.* The Alazami Syndrome-Associated Protein LARP7 Guides U6 Small
693 Nuclear RNA Modification and Contributes to Splicing Robustness. *Mol. Cell* (2020)
694 doi:10.1016/j.molcel.2020.01.001.

695 44. Wang, X. *et al.* LARP7-Mediated U6 snRNA Modification Ensures Splicing Fidelity and
696 Spermatogenesis in Mice. *Mol. Cell* (2020) doi:10.1016/j.molcel.2020.01.002.

697 45. Mitchell, J. R., Cheng, J. & Collins, K. A Box H/ACA Small Nucleolar RNA-Like Domain at
698 the Human Telomerase RNA 3' End. *Mol. Cell. Biol.* (1999) doi:10.1128/mcb.19.1.567.

699 46. Matera, A. G., Terns, R. M. & Terns, M. P. Non-coding RNAs: Lessons from the small
700 nuclear and small nucleolar RNAs. *Nature Reviews Molecular Cell Biology* (2007)

701 doi:10.1038/nrm2124.

702 47. Lafontaine, D. L. J., Bousquet-Antonelli, C., Henry, Y., Caizergues-Ferrer, M. & Tollervey,
703 D. The box H + ACA snoRNAs carry Cbf5p, the putative rRNA pseudouridine synthase.
704 *Genes Dev.* (1998) doi:10.1101/gad.12.4.527.

705 48. Tseng, C. K., Wang, H. F., Schroeder, M. R. & Baumann, P. The H/ACA complex disrupts
706 triplex in hTR precursor to permit processing by RRP6 and PARN. *Nat. Commun.* (2018)
707 doi:10.1038/s41467-018-07822-6.

708 49. Miyoshi, T., Kanoh, J., Saito, M. & Ishikawa, F. Fission yeast pot1-Tpp1 protects telomeres
709 and regulates telomere length. *Science (80-.).* (2008) doi:10.1126/science.1154819.

710 50. Shukla, S., Schmidt, J. C., Goldfarb, K. C., Cech, T. R. & Parker, R. Inhibition of telomerase
711 RNA decay rescues telomerase deficiency caused by dyskerin or PARN defects. *Nat.*
712 *Struct. Mol. Biol.* (2016) doi:10.1038/nsmb.3184.

713 51. Holohan, B. *et al.* Impaired telomere maintenance in Alazami syndrome patients with
714 LARP7 deficiency. *BMC Genomics* (2016) doi:10.1186/s12864-016-3093-4.

715 52. Singh, M. *et al.* Structural Basis for Telomerase RNA Recognition and RNP Assembly by
716 the Holoenzyme La Family Protein p65. *Mol. Cell* (2012)
717 doi:10.1016/j.molcel.2012.05.018.

718 53. Bähler, J. *et al.* Heterologous modules for efficient and versatile PCR-based gene
719 targeting in Schizosaccharomyces pombe. *Yeast* (1998) doi:10.1002/(SICI)1097-
720 0061(199807)14:10<943::AID-YEA292>3.0.CO;2-Y.

721 54. Oeffinger, M. *et al.* Comprehensive analysis of diverse ribonucleoprotein complexes. *Nat.*
722 *Methods* (2007) doi:10.1038/nmeth1101.

723 55. Vakiloroayaei, A., Shah, N. S., Oeffinger, M. & Bayfield, M. A. The RNA chaperone La
724 promotes pre-tRNA maturation via indiscriminate binding of both native and misfolded
725 targets. *Nucleic Acids Res.* **45**, 11341–11355 (2017).
726 56. Porat, J. & Bayfield, M. A. Use of tRNA-Mediated Suppression to Assess RNA Chaperone
727 Function. in *RNA Chaperones: Methods and Protocols* (ed. Heise, T.) 107–120 (Springer
728 US, 2020). doi:10.1007/978-1-0716-0231-7_6.
729 57. Bray, N. L., Pimentel, H., Melsted, P. & Pachter, L. Near-optimal probabilistic RNA-seq
730 quantification. *Nat. Biotechnol.* (2016) doi:10.1038/nbt.3519.
731 58. Robinson, J. T. *et al.* Integrative genomics viewer. *Nature Biotechnology* (2011)
732 doi:10.1038/nbt.1754.
733 59. Mukherjee, N., Lager, P. J., Friedersdorf, M. B., Thompson, M. A. & Keene, J. D.
734 Coordinated posttranscriptional mRNA population dynamics during T-cell activation. *Mol.*
735 *Syst. Biol.* (2009) doi:10.1038/msb.2009.44.
736 60. Cox, J. & Mann, M. MaxQuant enables high peptide identification rates, individualized
737 p.p.b.-range mass accuracies and proteome-wide protein quantification. *Nat. Biotechnol.*
738 (2008) doi:10.1038/nbt.1511.
739 61. Drissi, R., Dubois, M. L., Douziech, M. & Boisvert, F. M. Quantitative proteomics reveals
740 dynamic interactions of the minichromosome maintenance complex (MCM) in the
741 cellular response to etoposide induced DNA damage. *Mol. Cell. Proteomics* (2015)
742 doi:10.1074/mcp.M115.048991.
743 62. Kelley, L. A., Mezulis, S., Yates, C. M., Wass, M. N. & Sternberg, M. J. E. The Phyre2 web
744 portal for protein modeling, prediction and analysis. *Nat. Protoc.* (2015)

745 doi:10.1038/nprot.2015.053.

746 63. DeLano, W. L. The PyMOL Molecular Graphics System, Version 1.8. *Schrödinger LLC*

747 (2014) doi:10.1038/hr.2014.17.

748 64. Sievers, F. & Higgins, D. G. Clustal Omega. *Curr. Protoc. Bioinforma.* (2014)

749 doi:10.1002/0471250953.bi0313s48.

750 65. Buchfink, B., Xie, C. & Huson, D. H. Fast and sensitive protein alignment using DIAMOND.

751 *Nature Methods* (2014) doi:10.1038/nmeth.3176.

752 66. Miele, V., Penel, S. & Duret, L. Ultra-fast sequence clustering from similarity networks

753 with SiLiX. *BMC Bioinformatics* (2011) doi:10.1186/1471-2105-12-116.

754 67. Price, M. N., Dehal, P. S. & Arkin, A. P. FastTree 2 - Approximately maximum-likelihood

755 trees for large alignments. *PLoS One* (2010) doi:10.1371/journal.pone.0009490.

756 68. Mirarab, S. *et al.* ASTRAL: Genome-scale coalescent-based species tree estimation. in

757 *Bioinformatics* (2014). doi:10.1093/bioinformatics/btu462.

758 69. Perez-Riverol, Y. *et al.* The PRIDE database and related tools and resources in 2019:

759 Improving support for quantification data. *Nucleic Acids Res.* (2019)

760 doi:10.1093/nar/gky1106.

761

762

763

764

765

766

767

768

769

770

771

772

773

774 **Figure Legends:**

775

776 **Figure 1: Bin3 interacts with U6 snRNA and the telomerase RNA TER1**

777 A) Scatterplot of normalized and log-transformed Control IP TPM against Bin3 IP TPM. Bin3

778 targets of interest are indicated.

779 B) Northern blot analysis of the mature and intron-containing U6 from total RNA and PrA

780 immunoprecipitates from untagged (wild type, wt) and PrA-tagged Bin3 strains.

781 C) Same as (B), for the telomerase RNA TER1.

782

783 **Figure 2: Bin3 interacts with the same TER1 species as well-established components of the**

784 **telomerase holoenzyme**

785 A) The 5' and 3' ends of Bin3-, Trt1-, Pof8-, and Lsm3-associated TER1 were identified by cRACE.

786 The results of 10 independent clones per immunoprecipitation are shown below a schematic of

787 the architecture of TER1.

788 B) RNase H northern blots of RNase H generated 5’ and 3’ ends of TER1 immunoprecipitated by
789 various telomerase components.
790 C-D) Northern blot of α-TMG flow through (FT) and immunoprecipitated (IP) transcripts from
791 total RNA (C) and Bin3-associated transcripts (D).
792
793 **Figure 3: Bin3 interacts with components of the mature telomerase holoenzyme**
794 A) Gene ontology analysis (biological process) of top 50 Bin3 protein interactors.
795 B-C) Examination and nucleic acid-dependence of interactions between Bin3 and Pof8 (B) and
796 Bin3 and Trt1 (C) by co-immunoprecipitation and western blotting. Blots were reprobed for
797 beta actin as a loading control.
798
799 **Figure 4: Bin3 is recruited to the active telomerase holoenzyme by Pof8**
800 A) Northern blot of TER1 and U6 in PrA immunoprecipitates for an untagged wild type (wt),
801 PrA-tagged (Bin3 PrA), and PrA-tagged Pof8 knockout strain (Bin3 PrA ΔPof8). Bin3-PrA was
802 detected in input and immunoprecipitated samples by western blots probing for PrA (bottom
803 panel). Possible cleavage products are indicated with an asterisk.
804 B) Northern blot of mature and intron-containing U6 in PrA- and myc-tagged
805 immunoprecipitated RNA.
806 C) Telomerase assay of myc- (left) and PrA-tagged (right) proteins. A ^{32}P-labeled 100-mer
807 oligonucleotide was used as a loading control. Telomerase extension products were compared
808 to a terminal transferase ladder, with +1 and +6 extension products indicated.

809 D) Proposed model of the fission yeast telomerase holoenzyme. TER1 structure and binding

810 locations are based on models constructed by Hu and colleagues[15] and Mennie and

811 colleagues[13].

812

813 **Figure 5: Bin3 depletion results in an increase in TER1 levels and telomere length**

814 A) qRT-PCR of Bin3 mRNA normalized to his1 mRNA (mean ± standard error, paired *t* test *

815 at $p > 0.05$, ** at $p < 0.01$, *** at $p < 0.001$, and **** at $p<0.0001$).

816 B) qRT-PCR and a representative northern blot of TER1 from total cellular RNA (mean ±

817 standard error, paired *t* test * at $p > 0.05$, ** at $p < 0.01$, *** at $p < 0.001$, and **** at

818 $p<0.0001$).

819 C) Southern blot comparing telomere length in wild type, *pof8Δ*, and *bin3Δ* strains transformed

820 with an empty vector or GST-Bin3 following 2 re-streaks on minimal media with or without 15

821 μM thiamine (B1), as indicated.

822

823 **Figure 6: Phylogenic distribution of Bin3 and Pof8 in fungi**

824 Consensus cladogram describing the phylogenic relationships of 472 species representative of

825 fungi phylum and classes and highlighting (using a color code) the distribution of Bin3 and Pof8

826 in these species. The cladogram is a consensus tree of 5328 distinct protein coding gene trees

827 resulting from a genome-wide, against all, protein comparison (see Materials and Methods).

828 Only posterior probabilities inferior to 1 are shown. The Bin3 and Pof8 distribution is

829 recapitulated in Supplemental Table 8 with corresponding protein sequences. A cartoon

830 presenting structural domains of Pof8 is presented. Pof8 La module and RRM1 are only inferred

831 from secondary structure predictions and are represented by *La** and *RRM1** in the

832 corresponding cartoon. In four species (colored in orange in the cladogram) only an N-terminal

833 truncated version of Pof8 (Pof8*) that cannot accommodate the La module is present. Full

834 cladogram with species names and statistical supports of the different nodes is presented in

835 Figure S5.

836

837

838

839

840 **Supplementary figure captions:**

841

842 **Supplementary figure 1: Bin3 is the essential *S. pombe* methyl phosphate capping enzyme**

843 **(MePCE) homolog**

844 A) Clustal alignment of the methyltransferase/SAM-binding domains of *S. pombe* Bin3, *H.*

845 *sapiens* MePCE, and *D. melanogaster* Bin3. SAM-binding residues are indicated in red and

846 nucleotide-binding residues are in blue.

847 B) Phyre2 structure prediction [62] of *S. pombe* Bin3 bound to a 5' terminal guanosine (orange)

848 and SAH (green). Predicted SAM-binding residues are in red and nucleotide-binding residues

849 are in blue.

850 C) Wild type and Bin3 knockout strains transformed with pRep4x GST-Bin3 grown on minimal

851 media (EMM-ura) (left) and counter-selected on minimal media with 5'-fluoroorotic acid (right).

852 D) Bin3 overexpression results in a slow growth phenotype that is partially rescued with the

853 addition of thiamine (B1). 10-fold serial dilutions were plated on EMM-ura and grown at 32°C.

854

855 **Supplementary figure 2: Gaussian mixture modeling of the ratio histogram**

856 The posterior probabilities of associated Gaussian components for transcripts with a log of odds

857 greater than 3.17 are represented for the Bin3 IP (green line) and control IP (red line).

858

859

860

861 **Supplementary figure 3: Reciprocal co-immunoprecipitations validate an interaction between**

862 **Bin3 and Pof8**

863 The interaction between Bin3 and Pof8 was confirmed by α-myc co-immunoprecipitation.

864

865 **Supplementary figure 4: Bin3 overexpression fails to rescue *pof8Δ*-dependent telomere**

866 **defects**

867 Chromosome fusion PCR (top) from wild type and *pof8Δ* strains overexpressing the pRep4x

868 empty vector or pRep4x GST-Bin3. The Trt1 gene was amplified from genomic DNA as a loading

869 control (bottom).

870

871 **Supplementary figure 5: Phylogenetic distribution of Bin3 and Pof8 in fungi**

872 Complete consensus cladogram describing the phylogenic relationships of 472 species

873 representative of fungi phylum and classes and highlighting (using a color code) the distribution

874 of Bin3 and Pof8 in these species. Only posterior probabilities inferior to 1 are shown.

875

876

877

878

879

880

881

882

A

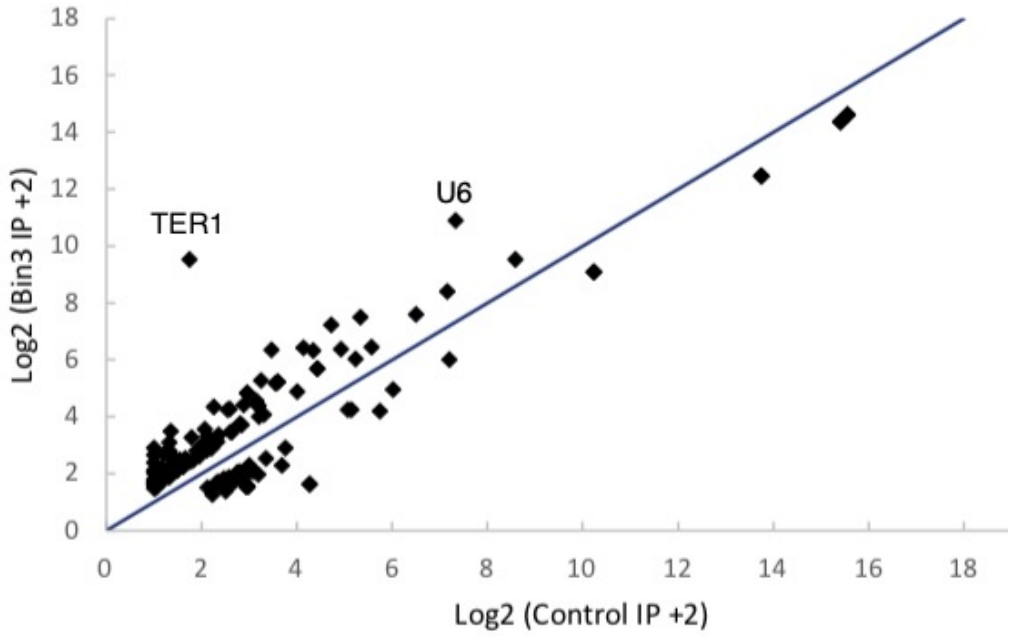
TER1
U6
Log2 (Bin3 IP +2)
Log2 (Control IP +2)
0
2
4
6
8
10
12
14
16
18

B

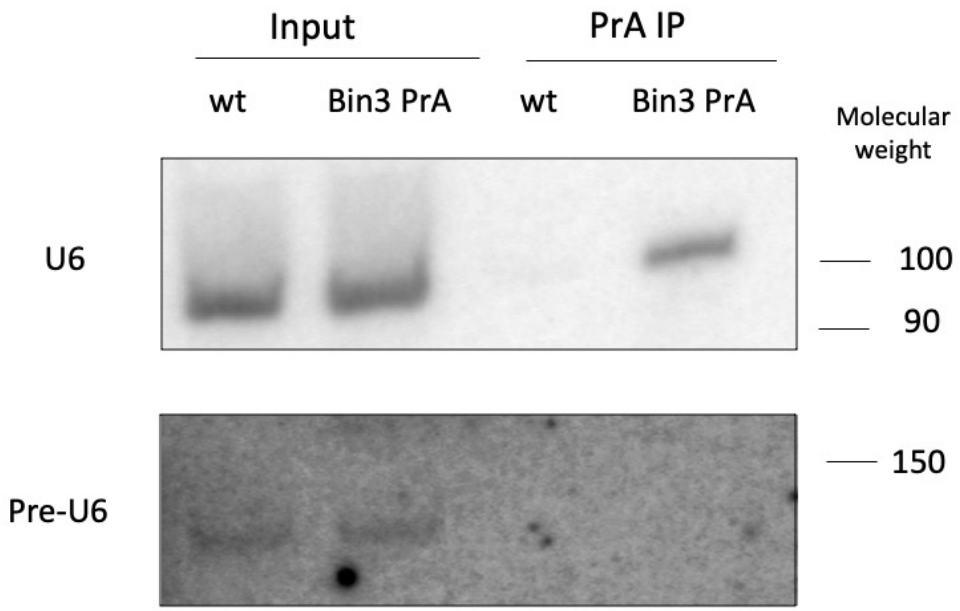
Input
PrA IP
wt
Bin3 PrA
wt
Bin3 PrA
Molecular weight
U6
100
90
Pre-U6
150

C

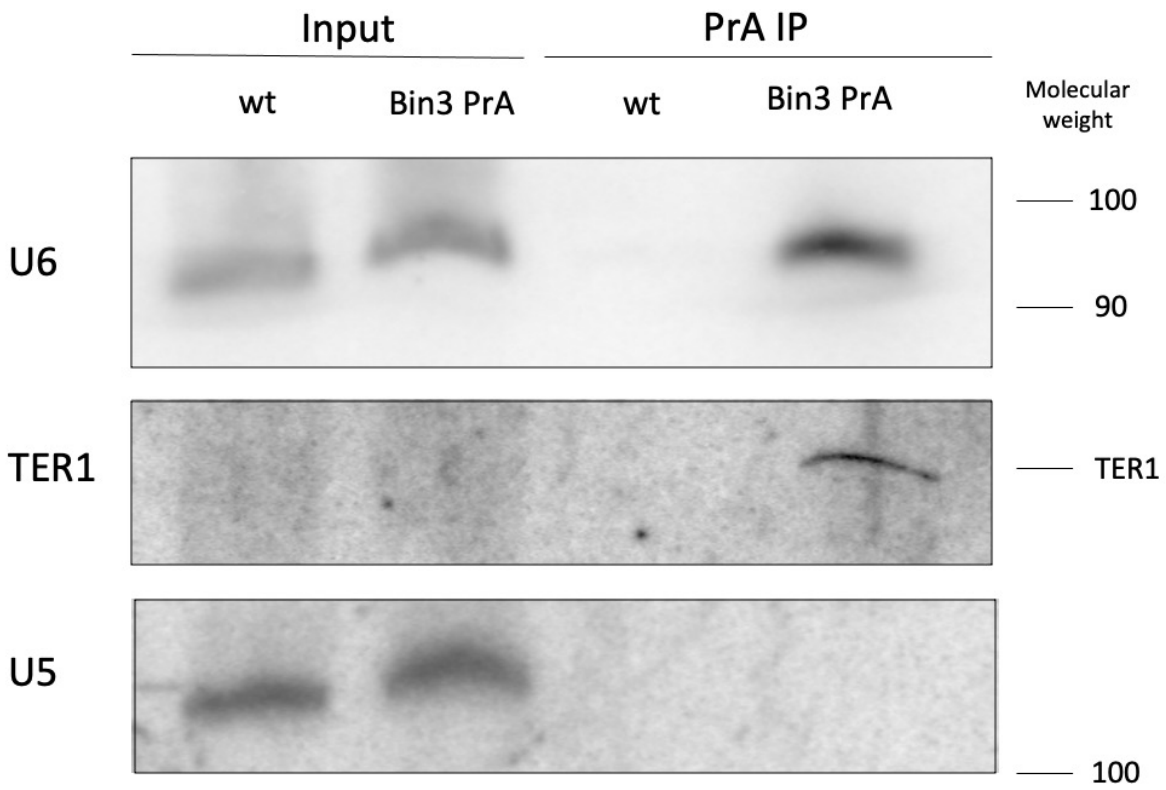
Input
PrA IP
wt
Bin3 PrA
wt
Bin3 PrA
Molecular weight
U6
100
90
TER1
TER1
U5
100

Figure 1: Bin3 interacts with U6 snRNA and the telomerase RNA TER1

A) Scatterplot of normalized and log-transformed Control IP TPM against Bin3 IP TPM. Bin3 targets of interest are indicated.

B) Northern blot analysis of the mature and intron-containing U6 from total RNA and PrA immunoprecipitates from untagged (wild type, wt) and PrA-tagged Bin3 strains.

C) Same as (B), for the telomerase RNA TER1.

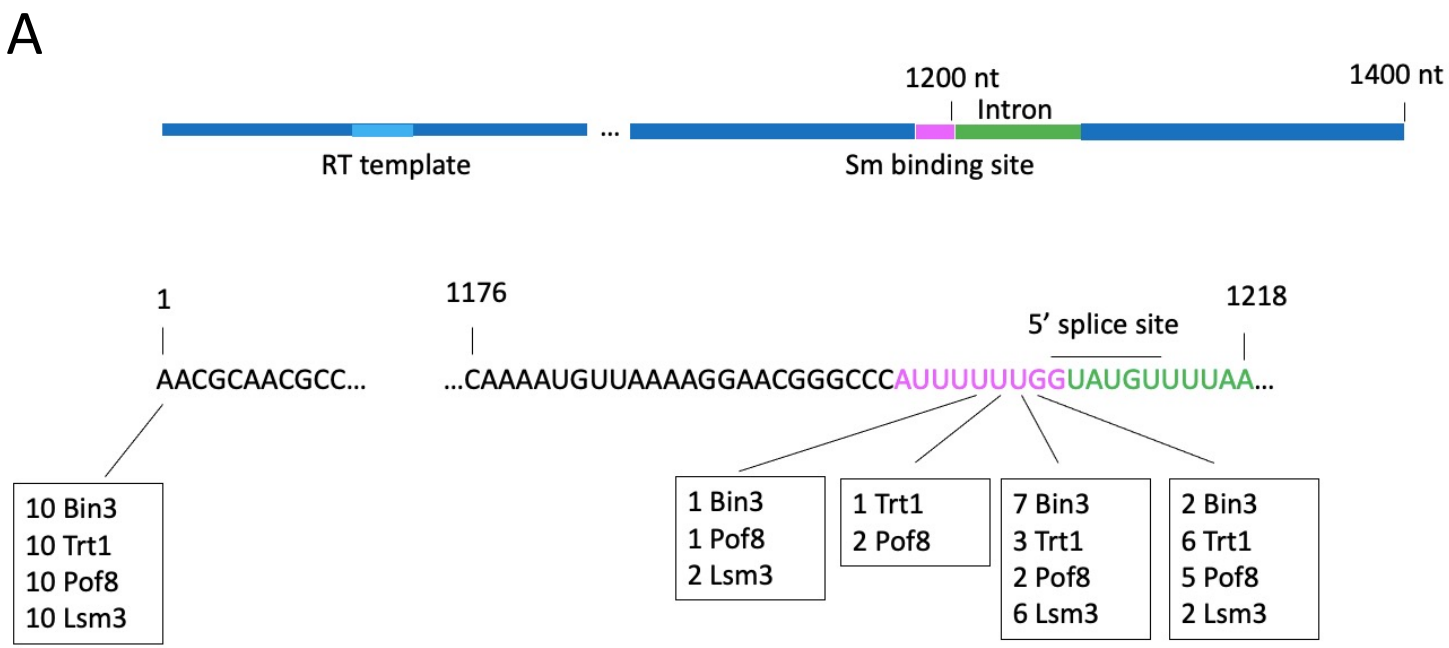
A
1200 nt
Intron
1400 nt
RT template
Sm binding site
1
1176
5' splice site
1218
AACGCAACGCC...
...CAAAAUGUUAAAAGGAACGGGCCCAUUUUUUGGUAUGUUUUAA...
10 Bin3
10 Trt1
10 Pof8
10 Lsm3
1 Bin3
1 Pof8
2 Lsm3
1 Trt1
2 Pof8
7 Bin3
3 Trt1
2 Pof8
6 Lsm3
2 Bin3
6 Trt1
5 Pof8
2 Lsm3

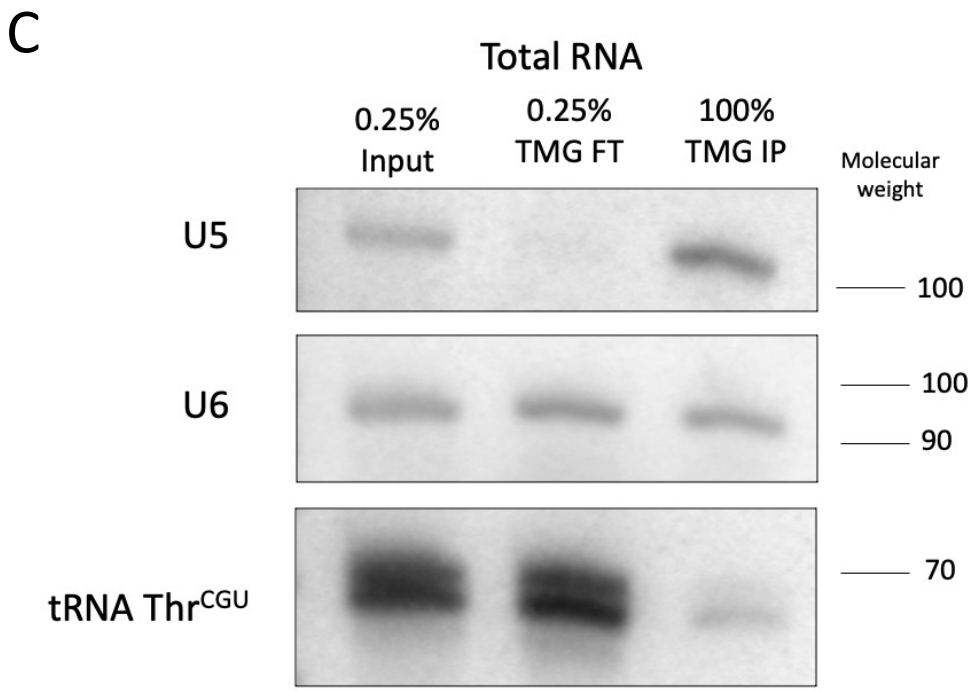
C
Total RNA
0.25% Input
0.25% TMG FT
100% TMG IP
Molecular weight
U5
100
U6
100
90
tRNA Thr^{CGU}
70

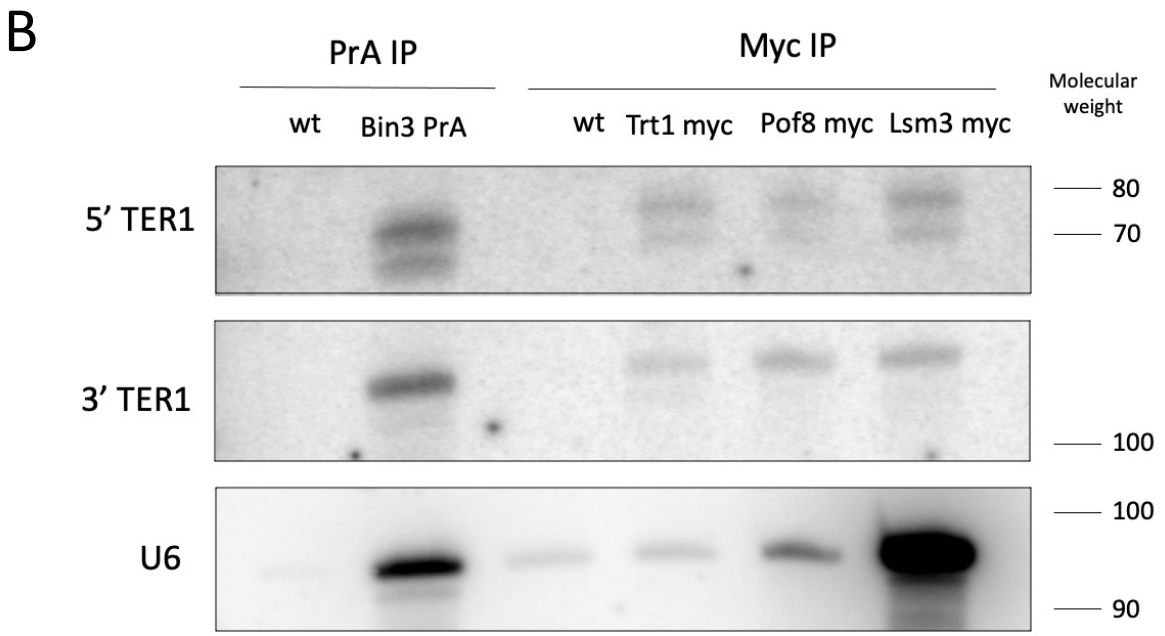
B
PrA IP
Myc IP
wt
Bin3 PrA
wt
Trt1 myc
Pof8 myc
Lsm3 myc
Molecular weight
5' TER1
80
70
3' TER1
100
U6
100
90

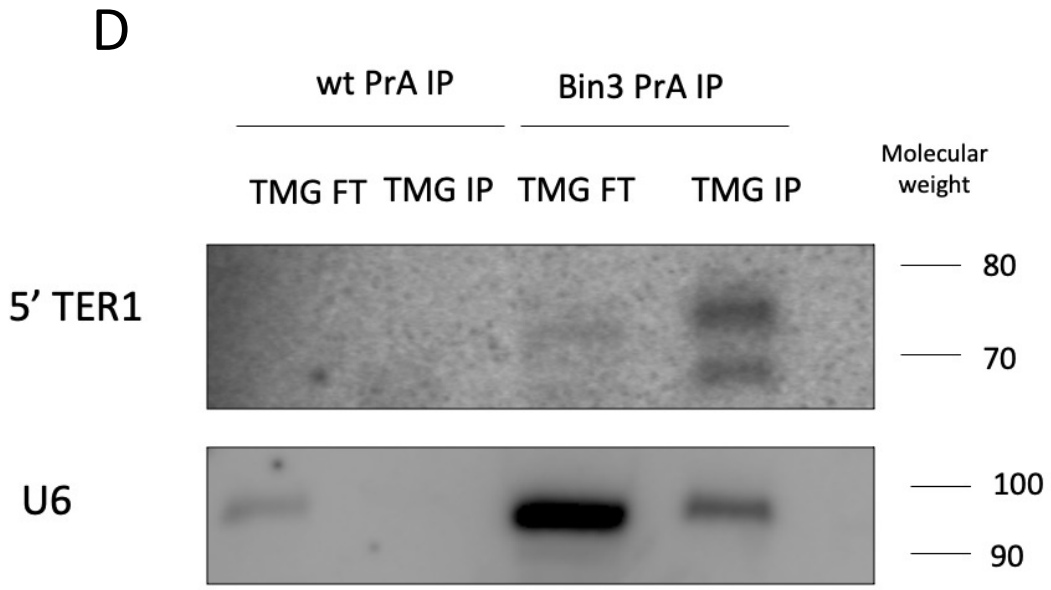
D
wt PrA IP
Bin3 PrA IP
TMG FT
TMG IP
TMG FT
TMG IP
Molecular weight
5' TER1
80
70
U6
100
90

Figure 2: Bin3 interacts with the same TER1 species as well-established components of the telomerase holoenzyme
A) The 5' and 3' ends of Bin3-, Trt1-, Pof8-, and Lsm3-associated TER1 were identified by cRACE. The results of 10 independent clones per immunoprecipitation are shown below a schematic of the architecture of TER1.
B) RNase H northern blots of RNase H generated 5' and 3' ends of TER1 immunoprecipitated by various telomerase components.
C-D) Northern blot of a-TMG flow through (FT) and immunoprecipitated (IP) transcripts from total RNA (C) and Bin3-associated transcripts (D).

A

GO biological process	Fold enrichment	Raw P value	False discovery rate
Telomerase holoenzyme complex assembly	49.39	2.04E-08	5.33E-05
Telomere maintenance via telomerase	31.75	2.54E-04	4.74E-02
RNA-dependent DNA biosynthetic process	31.75	2.54E-04	4.58E-02
Ribonucleoprotein complex assembly	5.47	6.70E-06	2.50E-03
Ribonucleoprotein complex subunit organization	5.29	9.01E-06	2.77E-03
mRNA cis splicing, via spliceosome	5.25	6.76E-05	1.54E-02
mRNA splicing, via spliceosome	4.78	5.48E-05	1.43E-02
RNA splicing, via transesterification reactions with bulged adenosine as nucleophile	4.78	5.48E-05	1.43E-02
RNA splicing, via transesterification reactions	4.72	6.08E-05	1.45E-02
RNA splicing	4.52	8.60E-05	1.80E-02

B

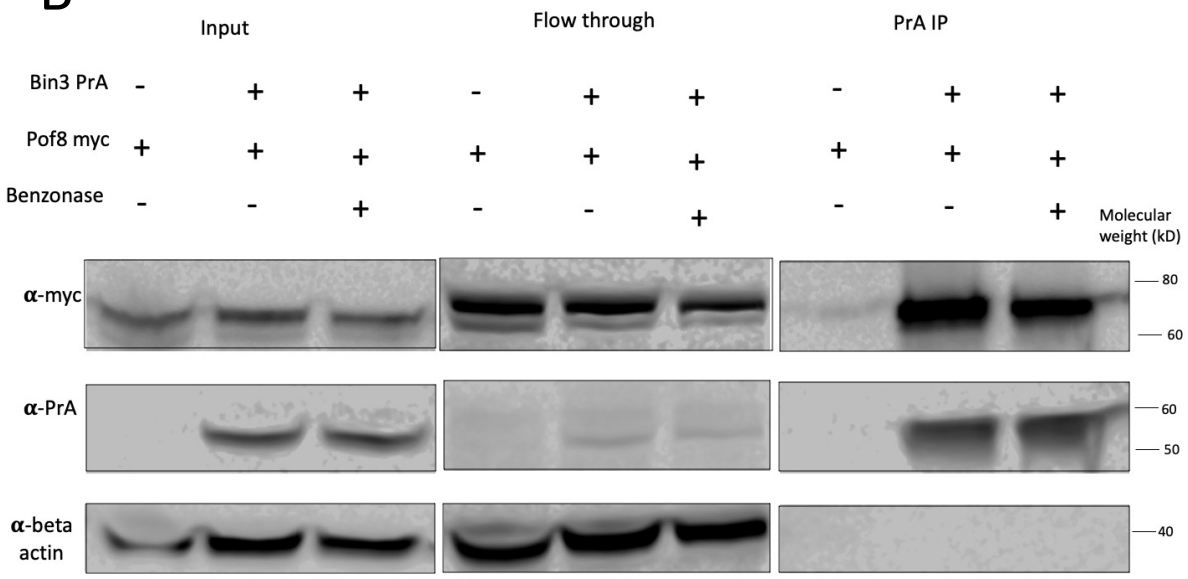

C

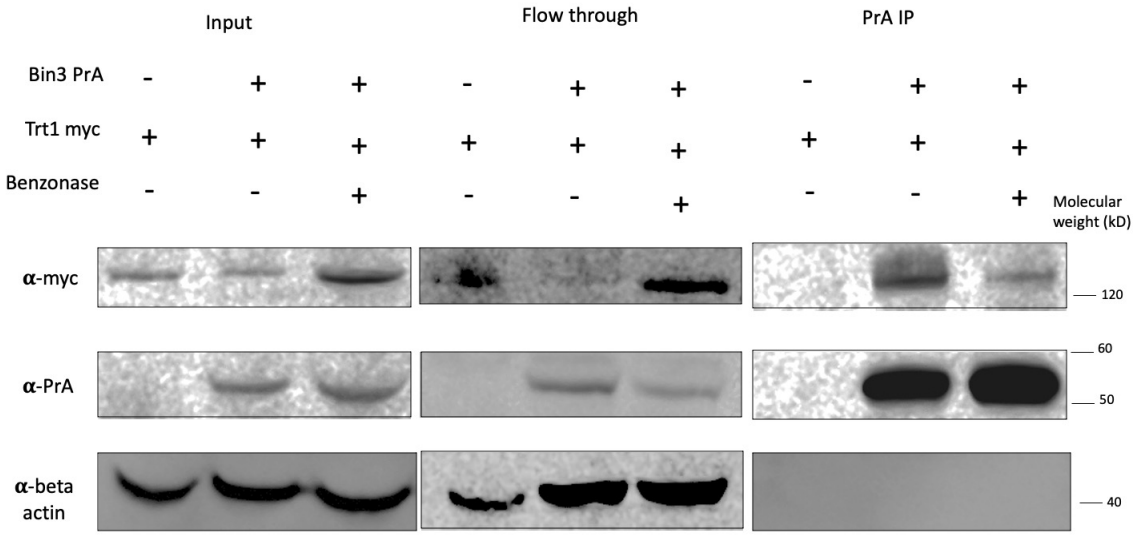

Figure 3: Bin3 interacts with components of the mature telomerase holoenzyme

A) Gene ontology analysis (biological process) of top 50 Bin3 protein interactors.

B-C) Examination and nucleic acid-dependence of interactions between Bin3 and Pof8 (B) and Bin3 and Trt1 (C) by co-immunoprecipitation and western blotting. Blots were reprobed for beta actin as a loading control.

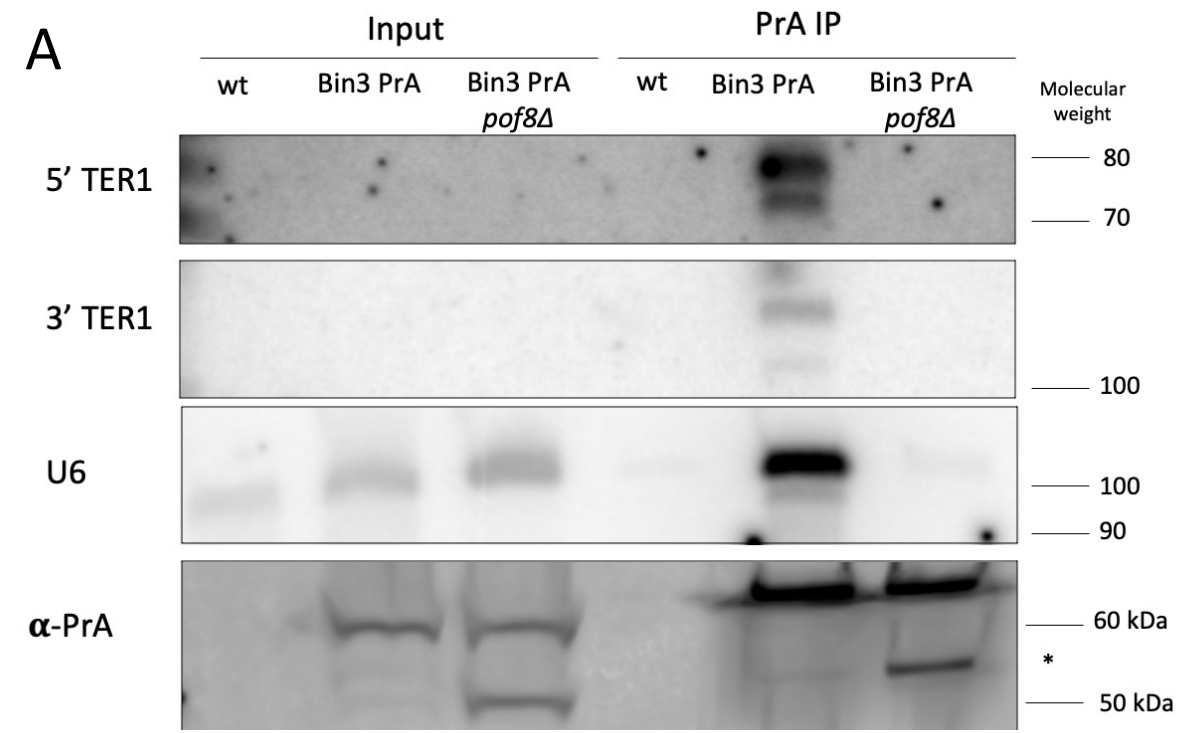
A
Input
PrA IP
wt
Bin3 PrA
Bin3 PrA pof8Δ
wt
Bin3 PrA
Bin3 PrA pof8Δ
Molecular weight
5' TER1
3' TER1
U6
α-PrA
80
70
100
100
90
60 kDa
*
50 kDa

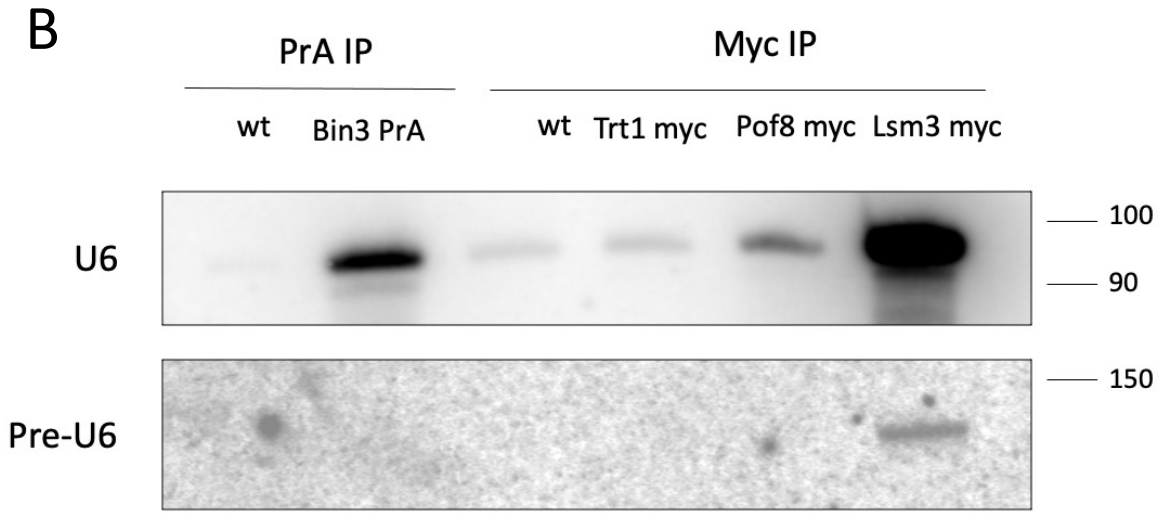
B
PrA IP
Myc IP
wt
Bin3 PrA
wt
Trt1 myc
Pof8 myc
Lsm3 myc
U6
Pre-U6
100
90
150

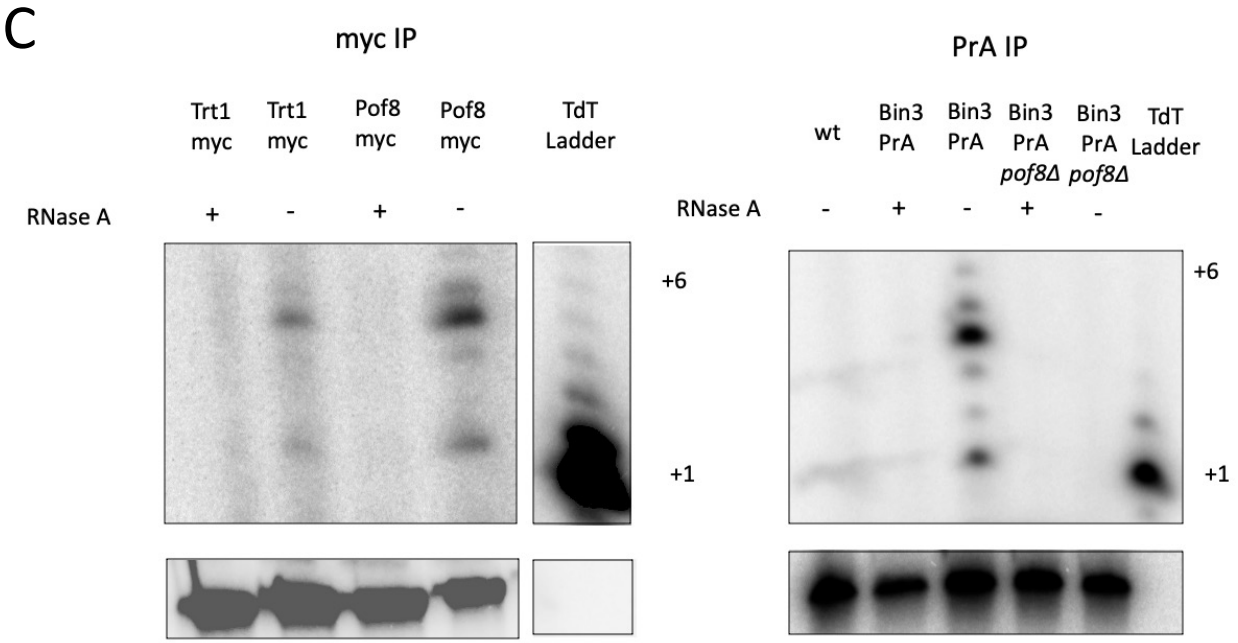
C
myc IP
Trt1 myc
Trt1 myc
Pof8 myc
Pof8 myc
TdT Ladder
RNase A
+
-
+
-
+6
+1
PrA IP
wt
Bin3 PrA
Bin3 PrA
Bin3 PrA pof8Δ
Bin3 PrA pof8Δ
TdT Ladder
RNase A
-
+
-
+
-
+6
+1

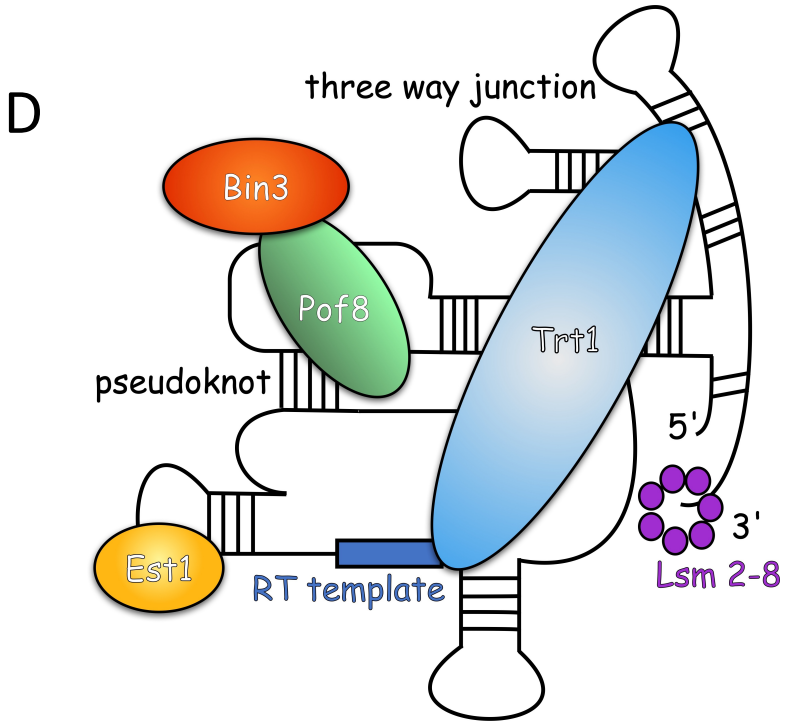
D
three way junction
Bin3
Pof8
Trt1
pseudoknot
5'
3'
Est1
RT template
Lsm 2-8

Figure 4: Bin3 is recruited to the active telomerase holoenzyme by Pof8

A) Northern blot of TER1 and U6 in PrA immunoprecipitates for an untagged wild type (wt), PrA-tagged (Bin3 PrA), and PrA-tagged Pof8 knockout strain (Bin3 PrA *pof8Δ*). Bin3-PrA was detected in input and immunoprecipitated samples by western blots probing for PrA (bottom panel). Possible cleavage products are indicated with an asterisk.

B) Northern blot of mature and intron-containing U6 in PrA- and myc-tagged immunoprecipitated RNA.

C) Telomerase assay of myc- (left) and PrA-tagged (right) proteins. A ^{32}P-labeled 100-mer oligonucleotide was used as a loading control. Telomerase extension products were compared to a terminal transferase ladder, with +1 and +6 extension products indicated.

D) Proposed model of the fission yeast telomerase holoenzyme. TER1 structure and binding locations are based on models constructed by Hu and colleagues[15] and Mennie and colleagues[13].

A

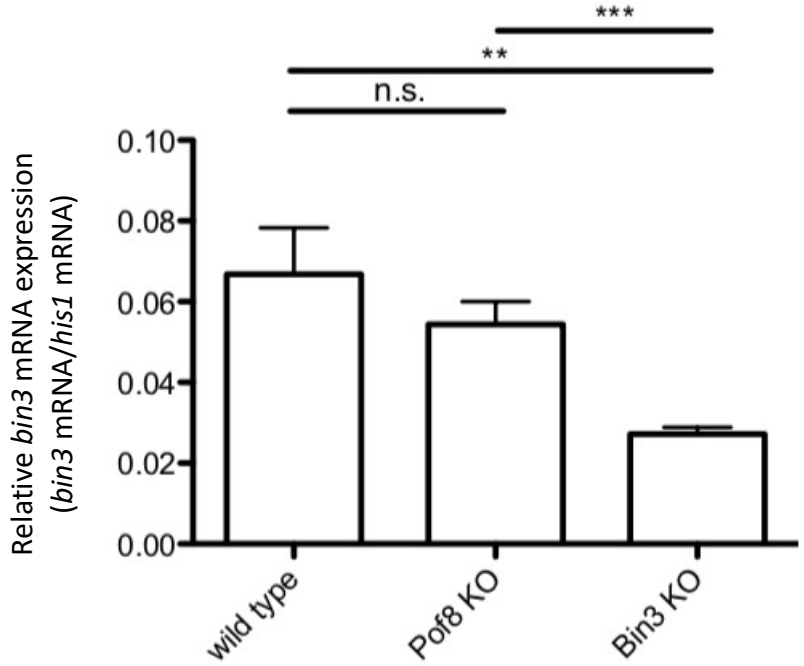
***
**
n.s.
Relative bin3 mRNA expression
(bin3 mRNA/his1 mRNA)
0.10
0.08
0.06
0.04
0.02
0.00
wild type
Pof8 KO
Bin3 KO

B

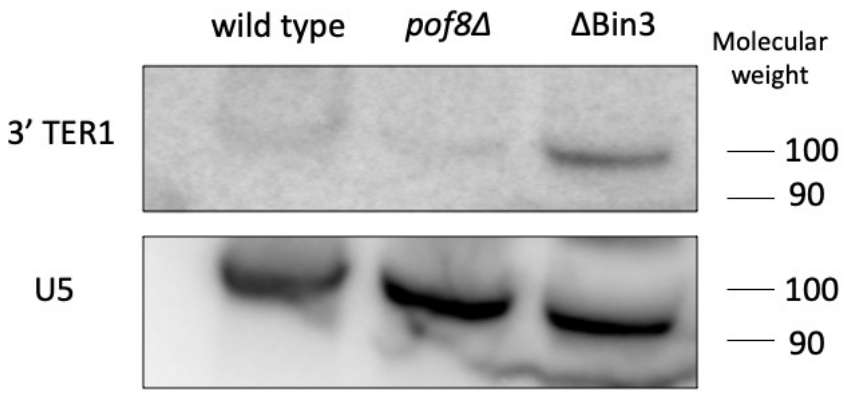
wild type
pof8Δ
ΔBin3
Molecular weight
3' TER1
100
90
U5
100
90

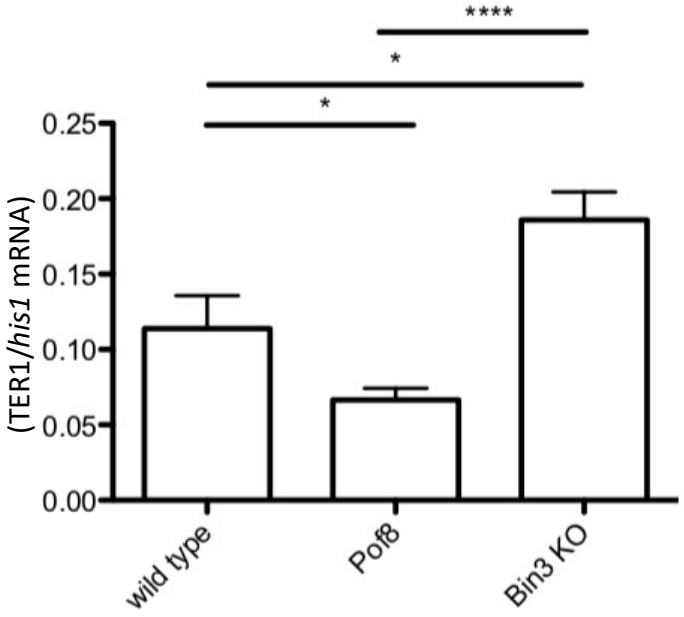
****
*
*
(TER1/his1 mRNA)
0.25
0.20
0.15
0.10
0.05
0.00
wild type
Pof8
Bin3 KO

C

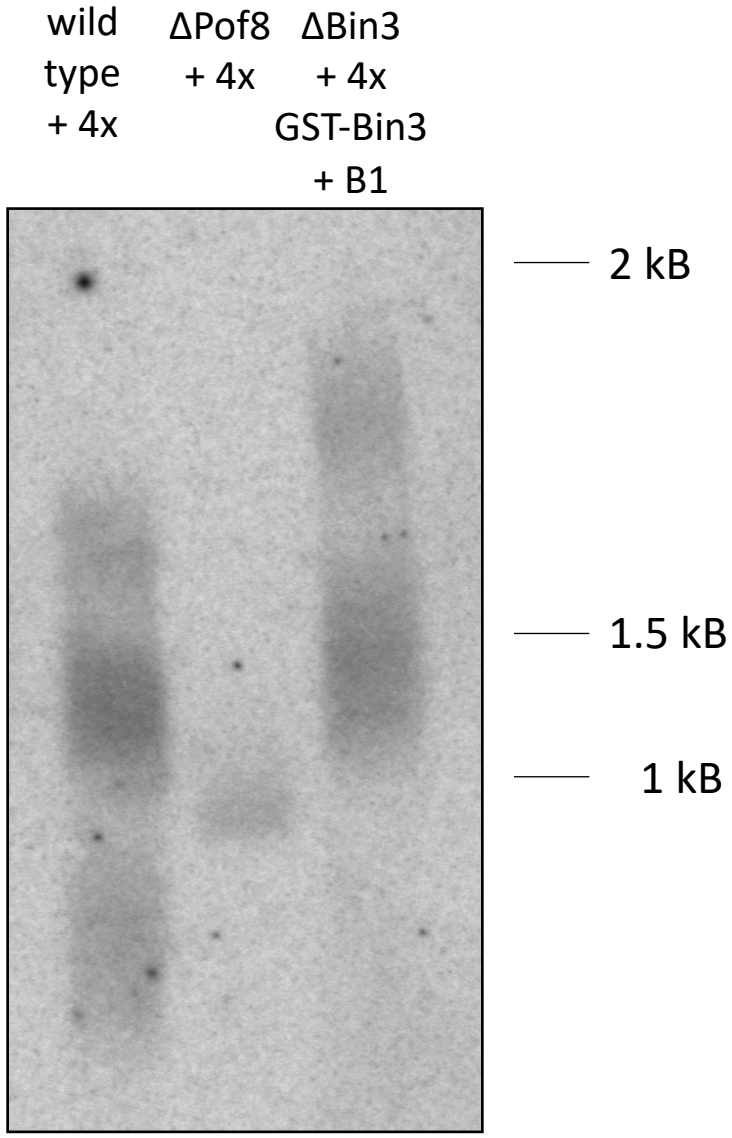
wild type + 4x
ΔPof8 + 4x
ΔBin3 + 4x GST-Bin3 + B1
2 kB
1.5 kB
1 kB

Figure 5: Bin3 depletion results in an increase in TER1 levels and telomere length

A) qRT-PCR of *bin3* mRNA normalized to *his1* mRNA (mean ± standard error, paired *t* test * at $p > 0.05$, ** at $p < 0.01$, *** at $p <$ paired *t* test * at $p > 0.05$, ** 0.001, and **** at $p<0.0001$).

B) qRT-PCR (normalized to *his1* mRNA) and a representative northern blot of TER1 from total cellular RNA (mean ± standard error, at $p < 0.01$, *** at $p < 0.001$, and **** at $p<0.0001$).

C) Southern blot comparing telomere length in wild type, ΔPof8, and ΔBin3 strains transformed with an empty vector or GST-Bin3 following 2 re-streaks on minimal media with or without 15 µM thiamine (B1), as indicated.

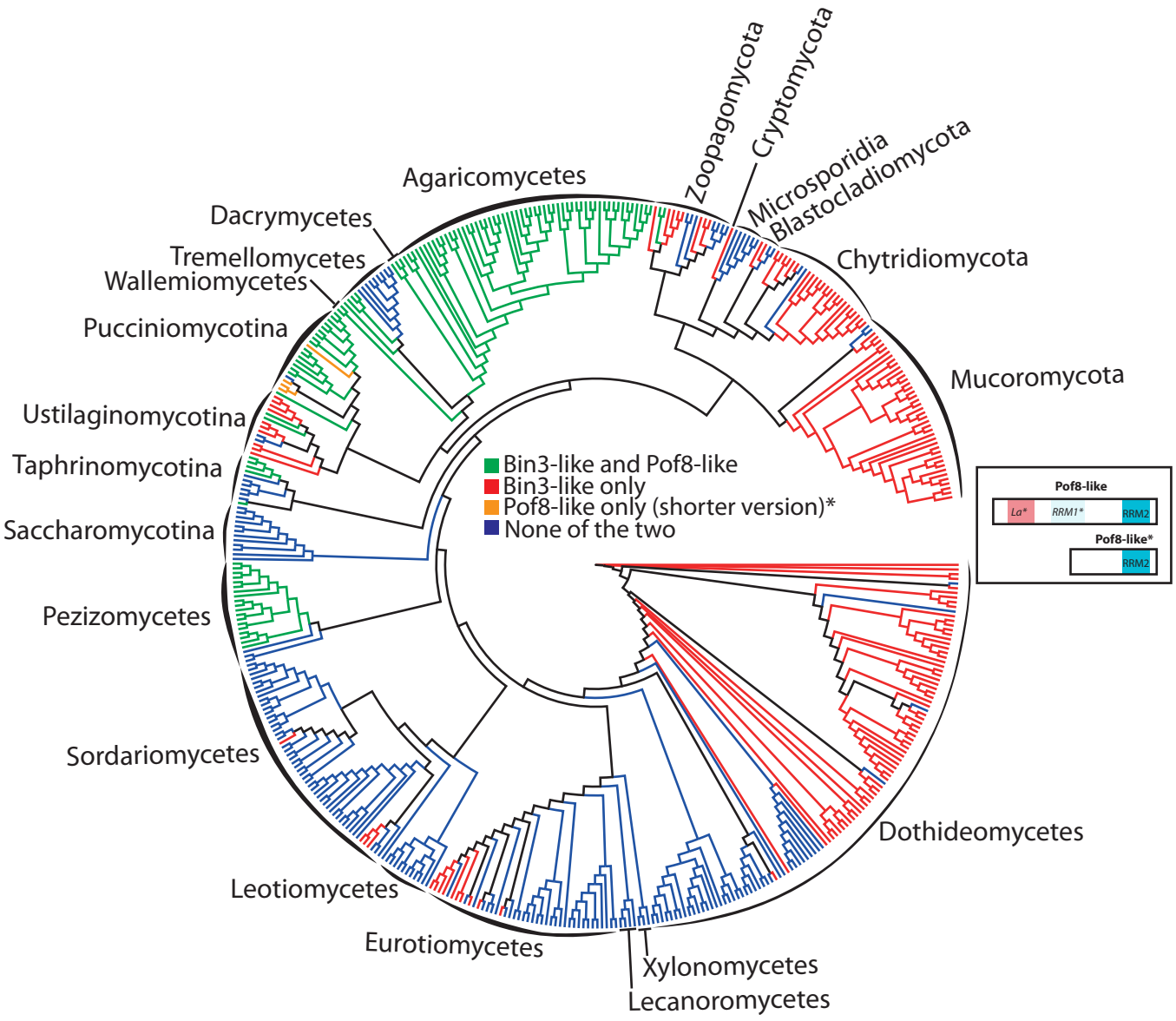
Zoopagomycota
Cryptomycota
Microsporidia
Blastocladiomycota
Chytridiomycota
Mucoromycota
Agaricomycetes
Dacrymycetes
Tremellomycetes
Wallemiomycetes
Pucciniomycotina
Ustilaginomycotina
Taphrinomycotina
Saccharomycotina
Pezizomycetes
Sordariomycetes
Leotiomycetes
Eurotiomycetes
Xylonomycetes
Lecanoromycetes
Dothideomycetes
Bin3-like and Pof8-like
Bin3-like only
Pof8-like only (shorter version)*
None of the two
Pof8-like
La*
RRM1*
RRM2
Pof8-like*
RRM2

Figure 6: Phylogenic distribution of Bin3 and Pof8 in fungi

Consensus cladogram describing the phylogenic relationships of 472 species representative of fungi phylum and classes and highlighting (using a color code) the distribution of Bin3 and Pof8 in these species. The cladogram is a consensus tree of 5328 distinct protein coding gene trees resulting from a genome-wide, against all, protein comparison (see Materials and Methods).

The Bin3 and Pof8 distribution is recapitulated in Supplemental Table 8 with corresponding protein sequences. A cartoon presenting structural domains of Pof8 is presented. Pof8 La module and RRM1 are only inferred from secondary structure predictions and are represented by *La** and *RRM1** in the corresponding cartoon. In four species (colored in orange in the cladogram) only an N-terminal truncated version of Pof8 (Pof8*) that cannot accommodate the La module is present. Full cladogram with species names and statistical supports of the different nodes is presented in Figure S5.

A

```
S.pombe          MSNFQHGNYHSYYSMRGGTSIIDPRLKCL--PDSLFYEASVLDIGCNNGTVSAQIASIFG    58
H.sapiens        --KFQYGNYCKYYGYRNPSC-EDGRLRVL--KPEWFRGRDVLDLGCNVGHLTLSIACKWG    55
D.melanogaster   --KYRYGNFDRYVDFRQMNEFRDVRLQVFQRHVELFENKDILDIGCNVGHMTITVARHLA    58
                   ::::**:  *. *  .   * **: :    . *   .:**:*** * ::  :*   .

S.pombe          ASFVLGLDIDHVLIQKARKHLEFVSSRIG---PV--------------------------    89
H.sapiens        PSRMVGLDIDSRLIHSARQNIRHYLSEELRLPPQTLEGDPGAEGEE--------------    101
D.melanogaster   PKTIVGIDIDRELVARARRNLSIFVRIPKEEKLLEVKAEPTVDAKANIAVKDETSGAAHK    118
                  . ::*:***  *:  **:::

S.pombe          ------------------------------RNPGSIVEDQFNYYPISSIKKFSRIPVQL    118
H.sapiens        ----------------------------------GTTTVRKRSCFPASLTASRGPI----    123
D.melanogaster   KTRRGKRRRKVHQGIHHHHHHHHDLEQLQQQQKLNSLLVKPHEFFPISFPLTYGRIPRIL    178
                                                  .:      . :* *   . . *

S.pombe          QPP------LNKQNFPHNIEFETADFLR------WESKRKFKIILALSVSKWVHLNNHDE    166
H.sapiens        AAPQVPLDGADTSVFPNNVVFVTGNYVLDRDDLVEAQTPEYDVVLCLSLTKWVHLNWGDE    183
D.melanogaster   SSSKSPNMLGNKNQFPANVFFRHTNYVLKDESLMASDTQQYDLILCLSVTKWIHLNFGDN    238
                            :.. ** *: *   :::         .. ::.::*.**:**:***  *:

S.pombe          GIIKFFGKISSLLETNGVLILEPQGWDSYLKAAKKISVFNQTPENLKIQPDAFEHLLNQA    226
H.sapiens        GLKRMFRRIYRHLRPGGILVLEPQPWSSYGKRKTLTETIYKNYYRIQLKPEQFSSYLTSP    243
D.melanogaster   GLKMAFKRMFNQLRPGGKLILEAQNWASYKKKKNLTPEIYNNYKQIEFFPNKFHEYLLSS    298
                 *:   * ::   *. .* *:** * * ** *  .    : :.  .::: *: *   * .

S.pombe          GLVLEYSIEPQVNNSEYKNFAKRTMYIYKKKGIGI-        261
H.sapiens        DVGFSSYELVATPHNTSKGFQ-RPVYLFHKARSPSH        278
D.melanogaster   EVGFSHSYTLGVPRHMNKGFC-RPIQLYAKGDYTPN        333
                  : :.      . .   * *  * : :: *
```

B

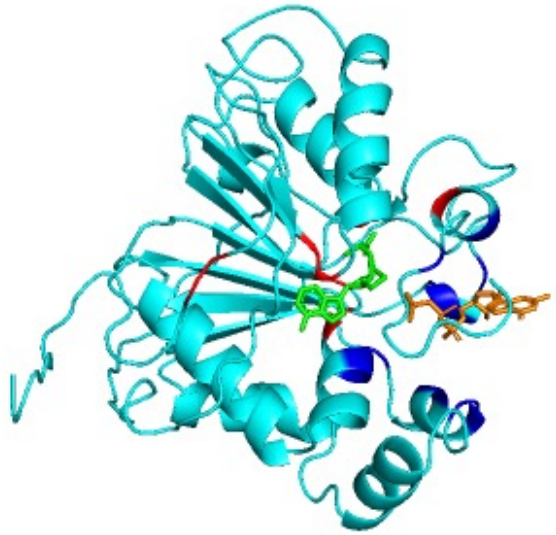

C

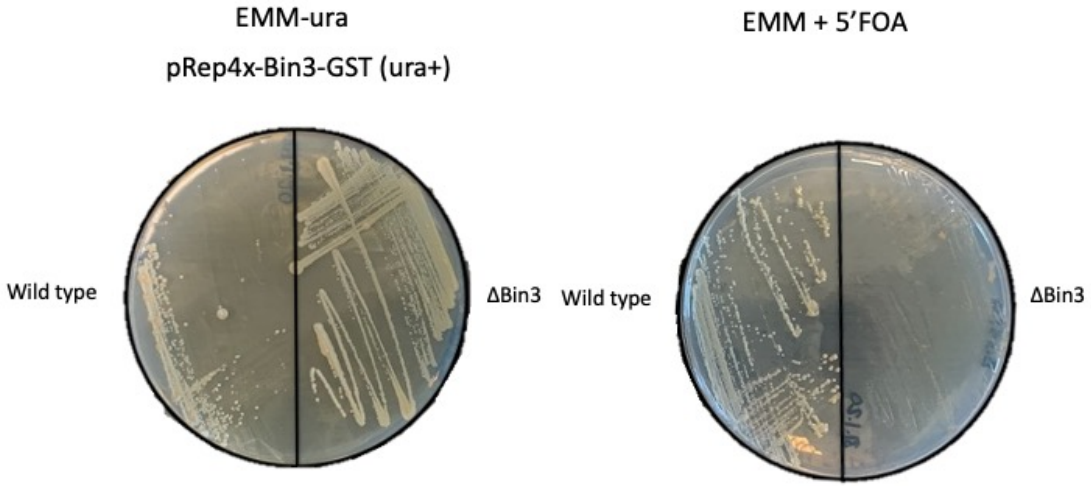

D

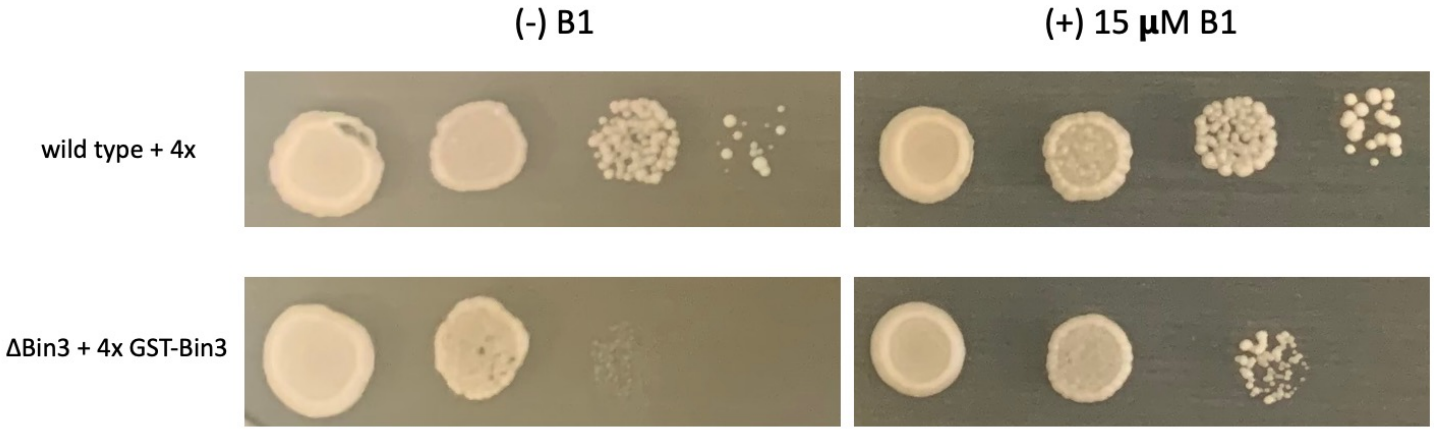

Supplementary figure 1: Bin3 is the essential *S. pombe* methyl phosphate capping enzyme (MePCE) homolog

A) Clustal alignment of the methyltransferase/SAM-binding domains of *S. pombe* Bin3, *H. sapiens* MePCE, and *D. melanogaster* Bin3. SAM-binding residues are indicated in red and nucleotide-binding residues are in blue.

B) Phyre2 structure prediction [62] of *S. pombe* Bin3 bound to a 5' terminal guanosine (orange) and SAH (green). Predicted SAM-binding residues are in red and nucleotide-binding residues are in blue.

C) Wild type and Bin3 knockout strains transformed with pRep4x Bin3 grown on minimal media (EMM-ura) (left) and counter-selected on minimal media with 5'-fluoroorotic acid (right).

D) Bin3 overexpression results in a slow growth phenotype that is partially rescued with the addition of thiamine (B1). 10-fold serial dilutions were plated on EMM-ura and grown at 32°C.

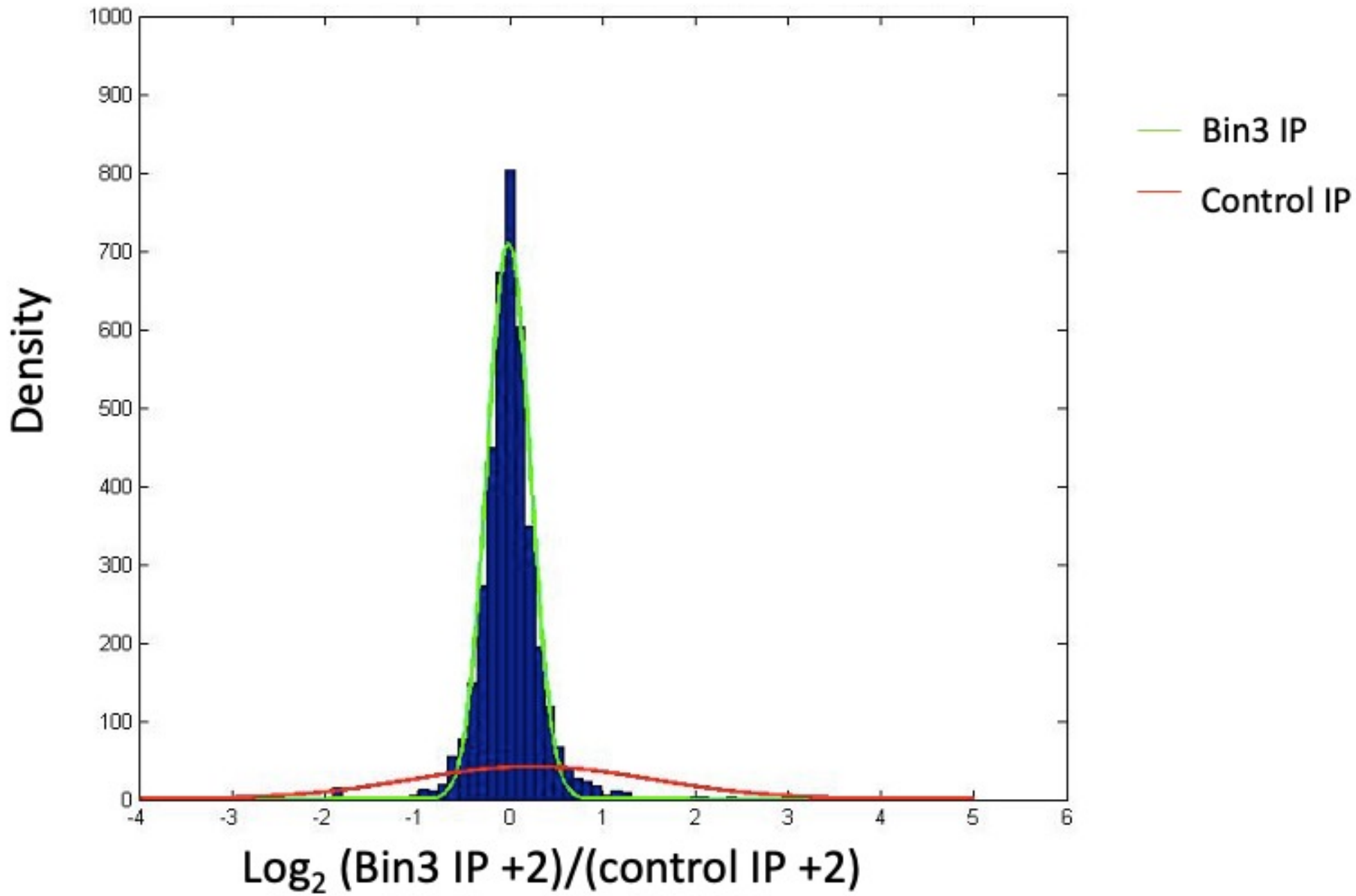
Density
1000
900
800
700
600
500
400
300
200
100
0
-4
-3
-2
-1
0
1
2
3
4
5
6
Log2 (Bin3 IP +2)/(control IP +2)
Bin3 IP
Control IP

Supplementary figure 2: Gaussian mixture modeling of the ratio histogram

The posterior probabilities of associated Gaussian components for transcripts with a log of odds greater than 3.17 are represented for the Bin3 IP (green line) and control IP (red line).

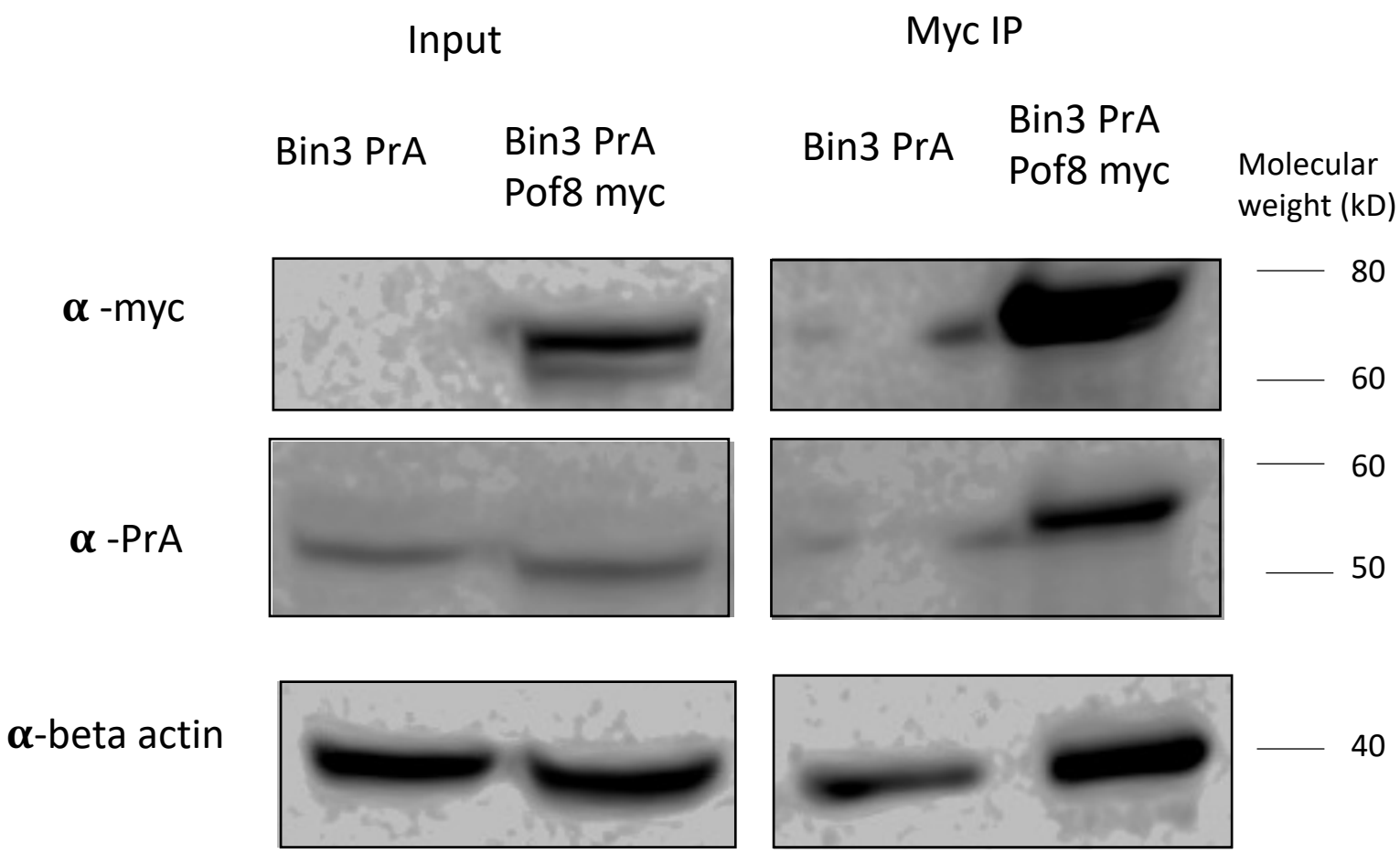
Input
Myc IP
Bin3 PrA
Bin3 PrA
Pof8 myc
Bin3 PrA
Bin3 PrA
Pof8 myc
Molecular
weight (kD)
α -myc
α -PrA
α-beta actin
80
60
60
50
40

Supplementary figure 3: Reciprocal co-immunoprecipitations validate an interaction between Bin3 and Pof8

The interaction between Bin3 and Pof8 was confirmed by α-myc co-immunoprecipitation.

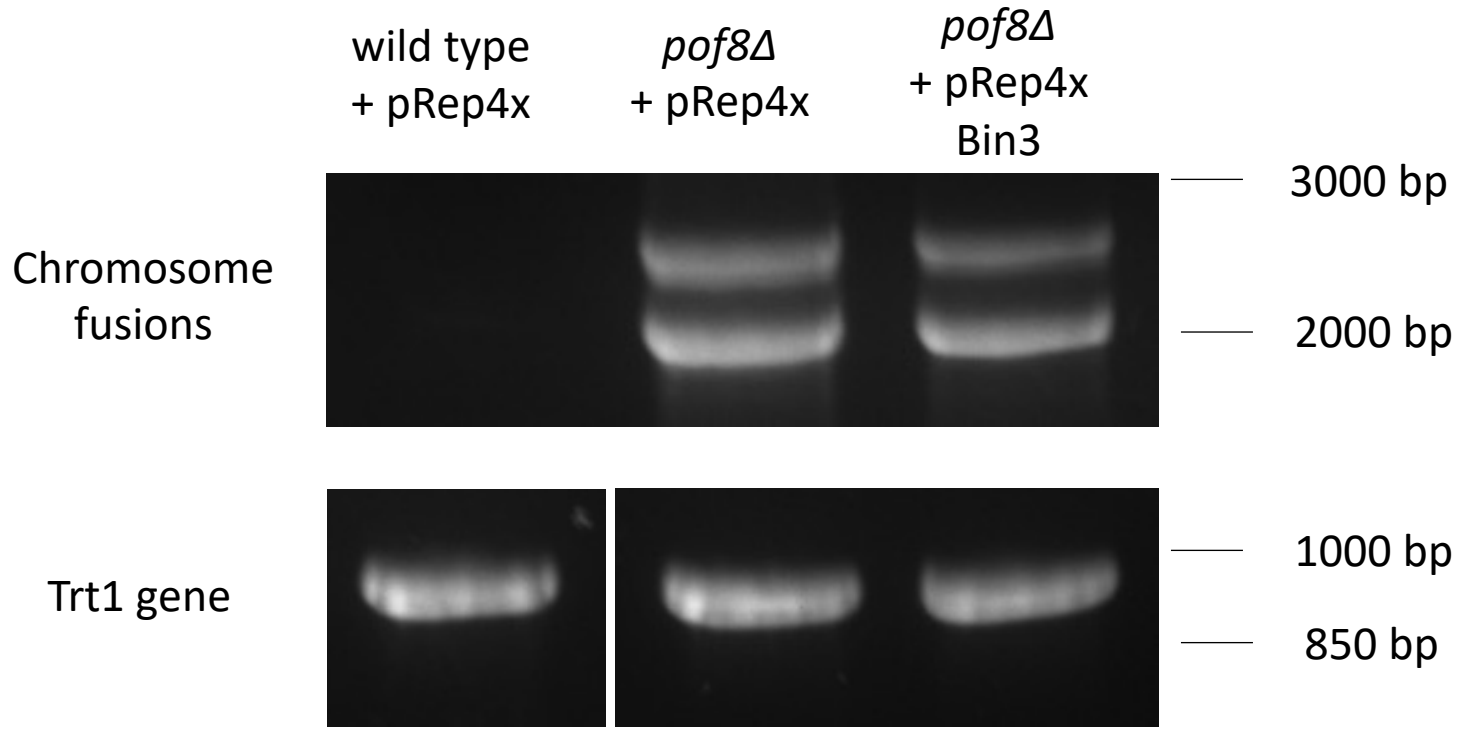
wild type
+ pRep4x
pof8Δ
+ pRep4x
pof8Δ
+ pRep4x
Bin3
Chromosome
fusions
3000 bp
2000 bp
Trt1 gene
1000 bp
850 bp

Supplementary figure 4: Bin3 overexpression fails to rescue *pof8Δ*-dependent telomere defects
Chromosome fusion PCR (top) from wild type and *pof8Δ* strains overexpressing the pRep4x empty vector or pRep4x Bin3. The Trt1 gene was amplified from genomic DNA as a loading control (bottom).

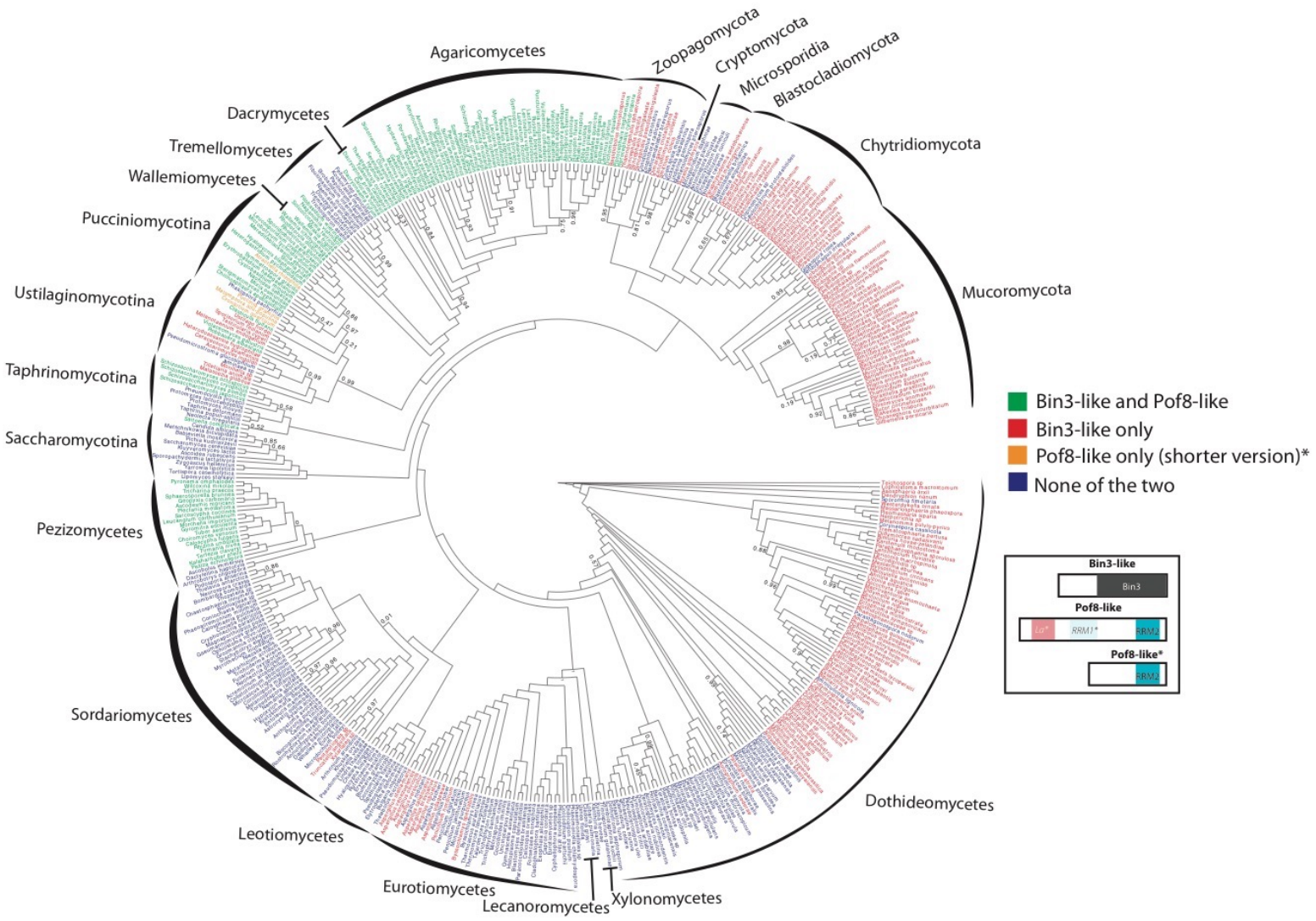
Agaricomycetes
Zoopagomycota
Cryptomycota
Microsporidia
Blastocladiomycota
Chytridiomycota
Mucoromycota
Dothideomycetes
Xylonomycetes
Lecanoromycetes
Eurotiomycetes
Leotiomycetes
Sordariomycetes
Pezizomycetes
Saccharomycotina
Taphrinomycotina
Ustilaginomycotina
Pucciniomycotina
Wallemiomycetes
Tremellomycetes
Dacrymycetes
Bin3-like and Pof8-like
Bin3-like only
Pof8-like only (shorter version)*
None of the two
Bin3-like
Bin3
Pof8-like
Lo*
RRM1*
RRM2
Pof8-like*
RRM2

Supplementary figure 5: Phylogenetic distribution of Bin3 and Pof8 in fungi

Complete consensus cladogram describing the phylogenic relationships of 472 species representative of fungi phylum and classes and highlighting (using a color code) the distribution of Bin3 and Pof8 in these species. Only posterior probabilities inferior to 1 are shown.

List of supplementary tables:

Supplementary table 1: Bin3-associated RNAs were detected by RIP-Seq (attached as spreadsheet)

Transcripts with 4 or more reads in at least one of the replicates, as well as a minimum log of odds value of 3.17, are presented.

Supplementary table 2: Results of Bin3-immunoprecipitated proteins from 2 independent mass spectrometry experiments

Proteins present exclusively in both replicates and absent from control immunoprecipitates were considered. The top 11 interacting proteins are presented, ranked by total peak intensity. Interactions persisting in the presence of benzonase are indicated. Experimentally validated and speculative components of the *S. pombe* telomerase holoenzyme are shaded.

Supplementary table 3: Top 50 Bin3-associated proteins used for GO analyses.

Supplementary table 4: Gene ontology analysis (cellular component) of the top 50 Bin3 protein interactors

Supplementary table 5: *S. pombe* strains used in this study

Supplementary Table 6: Primers used to generate tagged strains

Supplementary table 7: probe sequences

Supplementary Table 8: Distribution of Bin3 and Pof8 in the 472 species used to construct the cladogram of Figure 6 and corresponding protein sequences. (attached as spreadsheet)

Supplementary Table 9: Distribution of Bin3 and Pof8 in basal eukaryotic lineages. Presence of a Bin3- or LARP7-family member= Y, absence= N.

Supplementary Table 2

Protein	Gene	Bin3 PrA IP Replicate 1	Bin3 PrA IP Replicate 2	Bin3 PrA IP + benzonase
LARP7 family protein Pof8	pof8	24	24	22
Vigilin KH domain RNA binding protein	vgl1	17	14	20
Uncharacterized RNA binding protein	SPBC1861	16	24	0
RNase P and RNase MRP subunit Pop100	pop100	16	17	0
Telomerase reverse transcriptase Trt1	trt1	13	12	0
Bin3 family protein (bait)	SPBC2A9	12	12	11
WD repeat/ BOP1NT protein Erb1	erb1	9	9	1
Uncharacterized protein	SPCC18B5	7	7	7
Sec24/Sfb2 subunit	sec24	7	3	0
Telomerase regulator Est1	est1	6	9	0
Lsm2-8 complex subunit Lsm6	lsm6	6	6	0

Supplementary Table 3

Protein	Gene
LARP7 family protein Pof8	pof8
Bin3 family protein (bait)	SPBC2A9
Uncharacterized protein	SPCC18B5
Lsm2-8 complex subunit Lsm8	lsm8
Lsm2-8 complex subunit Lsm7	lsm7
Lsm2-8 complex subunit Lsm2	lsm2
Lsm2-8 complex subunit Lsm6	lsm6
Lsm2-8 complex subunit Lsm5	lsm5
Threonine tRNA ligase	ths1
RNase P and RNase MRP subunit Pop100	pop100
Periodic tryptophan protein 2 homolog	SPBC713

Vigilin KH domain RNA binding protein	vgl1
Uncharacterized RNA binding protein	SPBC1861
Putative glycine tRNA ligase	grs1
Small nuclear ribonucleoprotein-associated protein B	smb1
Pre-mRNA splicing factor Prp12	Prp1
Probable mitochondrial import receptor subunit Tom70	tom70
Nucleic acid binding protein homolog	byr3
Telomerase reverse transcriptase Trt1	trt1
Ribosome biogenesis protein Brx1	brx1
Ribosome biogenesis protein Erb1	erb1
Probable ATP-citrate synthase subunit 2	SPAC22A12

mRNA export factor Elf1	elf1
ATP synthase beta subunit 2	atp2
Sm snRNP core protein Smf1	smf1
Mitochondrial translation elongation factor EF-Tu	tuf1
CUE domain-containing protein	SPBC354
Putative G3BP-like protein	nxt3
Prp19 complex subunit	prp19
Vacuolar carboxypeptidase Y	cpy1
RNA binding protein Nop12	nop12
Putative mitochondrial ribosome recycling factor	tif451
U3 snoRNP-associated protein Utp7	utp7

Chaperonin-containing T-complex eta subunit	cct7
Telomerase regulator Est1	est1
BAR adaptor protein Hob3	hob3
Uncharacterized RNA binding protein	SPCC1827
RNA polymerase I upstream activation factor complex subunit Spp27	spp27
Uncharacterized RNA binding protein	SPBC4F6
Putative leucine-tRNA ligase Lrs1	lrs1
U5 snRNP complex subunit Spp42	spp42
DNA Polymerase V	pol5
Ribosome assembly factor, WD repeat protein Nsa1	nsa1
Translation initiation factor eIF2B epsilon subunit	tif225

26S protease regulatory subunit 8 homolog	let1

Supplementary Table 4

GO cellular component	Fold enrichment	Raw P value	False discovery rate
Lsm2-8 complex	42.34	8.86E-06	1.23E-03
Telomere holoenzyme complex	41.16	6.60E-07	2.44E-04
U6 snRNP	37.04	1.32E-05	1.63E-03
Spliceosomal tri-snRNP complex	15.88	4.49E-06	9.97E-04
U4/U6 x U5 tri-snRNP complex	15.88	4.49E-06	8.31E-04
Catalytic step 2 spliceosome	10.01	2.10E-04	1.46E-02
Spliceosomal snRNP complex	8.50	2.78E-05	2.80E-03
Small nuclear ribonucleoprotein complex	8.10	3.69E-05	3.42E-03
Sm-like protein family complex	7.98	4.05E-05	3.46E-03
Spliceosomal complex	6.12	7.25E-06	1.15E-03

Supplementary Table 5

Figure	Strain	Description	Full genotype	Source
1, Table S1	FY6843	wild type	*h- ura4-D18*	National BioResource Project
	yJP001	*bin3-PrA*	*h- ura4-D18 bin3^{+}::bin3-PrA-kanMX6*	This study
S1	yAS99	wild type	*h- leu1-32 ura4-D18 ade6-704*	Intine *et al.*, 2000 [70]
	yJP002	*bin3Δ + pRep4x GST-Bin3*	*h- leu1-32 ura4-D18 ade6-704 bin3Δ::natMX6 pRep4x GST-Bin3*	This study
2a, b	FY6843	wild type	*h- ura4-D18*	National BioResource Project
	yJP001	*bin3-PrA*	*h- ura4-D18 bin3^{+}::bin3-PrA-kanMX6*	This study
	TN7706	*trt1-myc*	*h- leu1-32 ura4-D18 his3-D1 trt1^{+}::G8-13myc-natMX6*	Mennie *et al.*, 2018
	AM16932	*pof8-myc*	*h- leu1-32 ura4-D18 his3-D1 pof8^{+}::13myc-kanMX6*	Mennie *et al.*, 2018
	AM17121	*lsm3-myc*	*h- leu1-32 ura4-D18 his3-D1 lsm3^{+}::13myc-kanMX6*	Mennie *et al.*, 2018
2c	FY6843	wild type	*h- ura4-D18*	National BioResource Project
	yJP001	*bin3-PrA*	*h- ura4-D18 bin3^{+}::bin3-PrA-kanMX6*	This study
3a, Table S2, Table S3, Table S4	FY6843	wild type	*h- ura4-D18*	National BioResource Project
	yJP001	*bin3-PrA*	*h- ura4-D18 bin3^{+}::bin3-PrA-kanMX6*	This study
3b, S3	yJP001	*bin3-PrA*	*h- ura4-D18 bin3^{+}::bin3-PrA-kanMX6*	This study
	yJP001a	*bin3-PrA*	*h+ ura4-D18 bin3^{+}::bin3-PrA-kanMX6*	This study
	yJP001b	*bin3-PrA*	*h+ ura4-D18 bin3^{+}::bin3-PrA-bleMX6*	This study
	AM16932	*pof8-myc*	*h- leu1-32 ura4-D18 his3-D1 pof8^{+}::13myc-kanMX6*	Mennie *et al.*, 2018

	yJP012	*bin3-PrA pof8-myc*	*h- leu1-32 ura4-D18 his3-D1 bin3^{+}::bin3-PrA-bleMX6 pof8^{+}::13myc-kanMX6*	This study
3c	yJP001	*bin3-PrA*	*h- ura4-D18 bin3^{+}::bin3-PrA-kanMX6*	This study
	yJP001a	*bin3-PrA*	*h+ ura4-D18 bin3^{+}::bin3-PrA-kanMX6*	This study
	yJP001b	*bin3-PrA*	*h+ ura4-D18 bin3^{+}::bin3-PrA-bleMX6*	This study
	TN7706	*trt1-myc*	*h- leu1-32 ura4-D18 his3-D1 trt1^{+}::G8-13myc-natMX6*	Mennie *et al.,* 2018
	yJP013	*bin3-PrA trt1-myc*	*h- leu1-32 ura4-D18 his3-D1 bin3^{+}::bin3-PrA-bleMX6 trt1^{+}::G8-13myc-natMX6*	This study
4a	FY6843	wild type	*h- ura4-D18*	National BioResource Project
	yJP001	*bin3-PrA*	*h- ura4-D18 bin3^{+}::bin3-PrA-kanMX6*	This study
	yJP001a	*bin3-PrA*	*h+ ura4-D18 bin3^{+}::bin3-PrA-kanMX6*	This study
	yJP001b	*bin3-PrA*	*h+ ura4-D18 bin3^{+}::bin3-PrA-bleMX6*	This study
	TN12118	*pof8Δ*	*h- leu1-32 ura4-D18 his3-D1 pof8Δ::kanMX6*	Mennie *et al.,* 2018
	TN12118a	*pof8Δ*	*h- leu1-32 ura4-D18 his3-D1 pof8Δ::natMX6*	This study
	yJP011	*bin3-PrA pof8Δ*	*h- leu1-32 ura4-D18 his3-D1 bin3^{+}::bin3-PrA-bleMX6 pof8Δ::natMX6*	This study
4b	FY6843	wild type	*h- ura4-D18*	National BioResource Project
	yJP001	*bin3-PrA*	*h- ura4-D18 bin3^{+}::bin3-PrA-kanMX6*	This study
	TN7706	*trt1-myc*	*h- leu1-32 ura4-D18 his3-D1 trt1^{+}::G8-13myc-natMX6*	Mennie *et al.,* 2018
	AM16932	*pof8-myc*	*h- leu1-32 ura4-D18 his3-D1 pof8^{+}::13myc-kanMX6*	Mennie *et al.,* 2018

	AM17121	*lsm3-myc*	*h- leu1-32 ura4-D18 his3-D1 lsm3^{+}::13myc-kanMX6*	Mennie *et al.,* 2018
4c	TN7706	*trt1-myc*	*h- leu1-32 ura4-D18 his3-D1 trt1^{+}::G8-13myc-natMX6*	Mennie *et al.,* 2018
	AM16932	*pof8-myc*	*h- leu1-32 ura4-D18 his3-D1 pof8^{+}::13myc-kanMX6*	Mennie *et al.,* 2018
	FY6843	wild type	*h- ura4-D18*	National BioResource Project
	yJP001	*bin3-PrA*	*h- ura4-D18 bin3^{+}::bin3-PrA-kanMX6*	This study
	yJP001a	*bin3-PrA*	*h+ ura4-D18 bin3^{+}::bin3-PrA-kanMX6*	This study
	yJP001b	*bin3-PrA*	*h+ ura4-D18 bin3^{+}::bin3-PrA-bleMX6*	This study
	TN12118	*pof8Δ*	*h- leu1-32 ura4-D18 his3-D1 pof8Δ::kanMX6*	Mennie *et al.,* 2018
	TN12118a	*pof8Δ*	*h- leu1-32 ura4-D18 his3-D1 pof8Δ::natMX6*	This study
	yJP011	*bin3-PrA pof8Δ*	*h- leu1-32 ura4-D18 his3-D1 bin3^{+}::bin3-PrA-bleMX6 pof8Δ::natMX6*	This study
5a, 5b, 5c	yAS99	wild type	*h- leu1-32 ura4-D18 ade6-704*	Intine *et al.,* 2000
	TN12118	*pof8Δ*	*h- leu1-32 ura4-D18 his3-D1 pof8Δ::kanMX6*	Mennie *et al.,* 2018
	yJP002	*BinΔ3 + pRep4x GST-Bin3*	*h- leu1-32 ura4-D18 ade6-704 bin3Δ::natMX6 pRep4x GST-Bin3*	This study
S4	FY6843	wild type	*h- ura4-D18*	National BioResource Project
	TN12118	*pof8Δ*	*h- leu1-32 ura4-D18 his3-D1 pof8Δ::kanMX6*	Mennie *et al.,* 2018

Supplementary Table 6

Primer	Sequence
Bin3 PrA For (tag integration)	5'CATTTGCTTAATCAAGCAGGACTAGTGCTTGAATACAGTATCGAACCTCA AGTAAATAACTCTGAGTACAAGAATTTTGCCAAACGAACAATGTATAAAAA AAAAGGAATTGGAATCATAAAACTATTAACTATTAACTTCTACTCGTACGCT GCAGGTCGAC 3'
Bin3 PrA Rev (tag integration)	5'CTACTTCATTCCGCTTTTCTTTCTTTCCTCATATGTTGAATTAGAGAATTTAAT AAAAAATGAGACACGTCCTTTTGGGACATTATGCTTTATAGTTCCAGTCATTGT CTATTCTTAACGTTTTACTAGACAAATCGATGAATTCGATGAATTCGAGCTCG 3'
MX6 For (antibiotic marker swap)	5' GACATGGAGGCCCAGAATAC 3'
MX6 Rev (antibiotic marker swap)	5' TGGATGCGCGCGTTAGTATC 3'
Bin3 KO For (Bin3 gene disruption)	5'TTCGATTCGTAAGTTTAAATTCCATTGCAAAATTTATACTTTTATAAAAAATA GGGGTGATTTGAAAAACCTCCTCGACTTGGGCGGATCCCCGGGTTAATTAA 3'
Bin3 KO Rev (Bin3 gene disruption)	5'GAGAATTTAATAAAAAATGAGACACGTCCTTTTGGGACATTATGCTTTATA GTTCCAGTCATTGTCTATTCTTAACGTTTTACTAGACAAGAATTCGAGCTCGTT TAAAC 3'

Supplementary Table 7

Figure	Probe	Sequence
1c, 1d, 2b, 3c, 2d, 4a, 4b	U6	5’ GTGTCATCCTTGTGCAGGGGCCAT 3’
1c, 4b	U6 intron	5’ CAACGAGTTAGTATGACTCGAACCTTGG 3’
1d	Ter1	5’ CCCGTTCCTTTTAACATTTTGCTCAGACCAAGTG 5’
1d, 2c, 5b	U5	5’ CTGGTAAAAGGCAAGAAACAGATACG 3’
2a	Ter1 cRACE For	5’ TCTTGAGCGCGTTTTAGGTTTTTTTCACTT 3’
	Ter1 cRACE Rev	5’ AACAACGGACGAGCTACACTCAAAATATTA 3’
2b, 4a, 4b, 5b	Ter1 3’ RNase H	5’ GGGTAGTCAACTATTTTACTAGCG 3’
	Ter1 5’ RNase H	5’ TTTCAAATCAATCACCAAGCCC 3’
	Ter1 3’ RNase H northern	5’ GCTCAGACCAAGTGAAAAAAACC 3’
	Ter1 5’ RNase H northern	5’ TCCTTGTCAACCTTCTAAGCATG 3’
2c	tRNA Thr^{CGU}	5’ TGCTCCGGCAGTGACTCGAACA 3’
4c	Telomerase assay primer	5’ GTTACGGTTACAGGTTACG 3’
5a	Bin3 mRNA 5’ qPCR	5’ GAGGAACCTCAATTATCGATCCAAGACTTAAATGTTTGC 3’
	Bin3 mRNA 3’ qPCR	5’ TCGAGCTTTTTGGATGAGAACATGATCGATATCCAATCC 3’
	His1 5’ qPCR	5’ TGTCCACCTCGGAATCACTG 3’
	His1 3’ qPCR	5’ CGAAGACGTGCTTCAGCGA 3’
5b	Ter1 5’ qPCR	CAGTGTACGTGAGTCTTCTGCCTT
	Ter1 3’ qPCR	CAAAAATTCGTTGTGATCTGACAAG
5c	Telomere southern probe	5’ GGGTTACATGTTACAGGTTACA 3’
S3	Chromosome fusion For	5’ GGGTTGCAAAGTATGATTGTGGTAA 3’
	Chromosome fusion Rev	5’ TGTTGAATGTCAGAACCAACTGTTGCAT 3’
	Trt1 For	5’ GCAAAGAAGTTTCCTGGAATAGC 3’
	Trt1 Rev	5’ GATGTAATAAAGGGTCGGCAC 3’

Supplementary Table 9

Species	Classification	BIN3	LARP7
Fragilariopsis cylindrus	Stramenopiles, Bacillariophyta	N	N
Pseudo-nitzschia multiseries	Stramenopiles, Bacillariophyta	N	N
Thalassiosira oceanica	Stramenopiles, Bacillariophyta	N	N
Thalassiosira pseudonana	Stramenopiles, Bacillariophyta	N	N
Ochromonadaceae sp	Stramenopiles, Chrysophyta	Y	N
Nannochloropsis gaditana	Stramenopiles, Eustigmatophyceae	Y	N
Nannochloropsis oceanica	Stramenopiles, Eustigmatophyceae	Y	N
Aplanochytrium kerguelense	Stramenopiles, Labyrinthulomycetes	N	N
Aurantiochytrium limacinum	Stramenopiles, Labyrinthulomycetes	N	N
Schizochytrium aggregatum	Stramenopiles, Labyrinthulomycetes	N	N
Achlya hypogyna	Stramenopiles, Oomycota	Y	Y
Aphanomyces euteiches	Stramenopiles, Oomycota	Y	Y
Aphanomyces astaci	Stramenopiles, Oomycota	Y	Y
Phytophthora cactorum	Stramenopiles, Oomycota	y	y
Phytophthora capsici	Stramenopiles, Oomycota	y	y
Phytophthora cinnamomi	Stramenopiles, Oomycota	y	y
Phytophthora infestans	Stramenopiles, Oomycota	y	y
Phytophthora sojae	Stramenopiles, Oomycota	y	y
Plasmopara halstedii	Stramenopiles, Oomycota	y	y
Pythium brassicum	Stramenopiles, Oomycota	Y	Y
Saprolegnia parasitica	Stramenopiles, Oomycota	Y	Y
Thraustotheca clavata	Stramenopiles, Oomycota	Y	Y
Blastocystis hominis	Stramenopiles, Opalozoa	N	N
Pelagophyceae sp.	Stramenopiles, Pelagophyceae	Y	Y
Ectocarpus siliculosus	Stramenopiles, Phaeophyceae	Y	Y
Tetrahymena thermophila	Alveolates, Ciliophora	Y	Y
Paramecium tetraurelia	Alveolates, Ciliophora	Y	Y
Pseudocohnilembus persalinus	Alveolates, Ciliophora	Y	N
Oxytricha trifallax	Alveolates, Ciliophora	Y	Y
Symbiodinium microadriaticum	Alveolates, Dinophyta	Y	N
Stylonychia lemnae	Alveolates, Ciliophora	Y	Y
Stentor coeruleus	Alveolates, Ciliophora	Y	N
Perkinsus marinus	Alveolates, Perkinsea	Y	N
Vitrella brassicaformis	Alveolates, Chromorida	Y	N
Gregarina niphandrodes	Alveolates, Apicomplexa	N	N
Cryptosporidium muris	Alveolates, Apicomplexa	N	N
Eimeria acervulina	Alveolates, Apicomplexa	Y	N

Toxoplama gondii	Alveolates, Apicomplexa	Y	N
Neospora caninum	Alveolates, Apicomplexa	Y	N
Cyclospora cayetanensis	Alveolates, Apicomplexa	N	N
Cystoisospora suis	Alveolates, Apicomplexa	Y	N
Plasmodiophora brassicae	Rhizaria, Endomixa	Y	N
Trypanosoma brucei	Excavates, Euglenozoa	N	N
Naegleria gruberi	Excavates, Heterolobosea	Y	N
Naegleria fowleri	Excavates, Heterolobosea	Y	N
Giardia lamblia	Excavates, Fornicata	N	N
Giardia intestinalis	Excavates, Fornicata	N	N
Trichomonas vaginalis	Excavates, Parabasalia	N	N
Emiliania huxleyi	Haptophyta, Isochrysidales	Y	Y
Chrysochromulina tobinii	Haptophyta, Prymnesiales	N	N
Pavlovalas sp	Haptophyta, Pavlovales	Y	N
Phaeocystis globosa	Haptophyta, Phaeocystales	Y	N